RSC Advances

REVIEW

View Article Online
View Journal | View Issue

Cite this: *RSC Adv.*, 2024, **14**, 33843

Crosslinked polymeric networks of TiO_2–polymer composites: a comprehensive review

Muhammad Arif, *[a] Mohsin Javed[a] and Toheed Akhter *[b]

Received 25th September 2024
Accepted 8th October 2024

DOI: 10.1039/d4ra06922f

rsc.li/rsc-advances

The crosslinked network of TiO_2–organic polymer composites has gained considerable attention over the past few years. The low band gap of TiO_2 particles and the stimuli–responsive behavior of organic polymers make these composites suitable for a wide range of applications in biomedicine, environmental fields, and catalysis. Diverse morphologies and structures of TiO_2–polymer composites (TPCs) are documented in the available literature, where the specific architecture of these composites intensely influences their efficiency in various applications. Consequently, a particular shaped TPC is carefully designed to suit specific purposes. This comprehensive review describes the classifications, synthetic approaches, characterizations, and applications of TiO_2 nanoparticles decorated in crosslinked organic polymers. It delves into the biomedical, catalytic, adsorption, and environmental applications of these TiO_2–polymer composites. The review takes a tutorial approach, systematically exploring and clarifying the applications of TiO_2–polymer composites, offering a comprehensive understanding of their different capabilities and uses.

1. Introduction

Since the advent of composite materials in the early 1970s, researchers worldwide have been struggling to develop materials that accurately and precisely meet the requirements of applications.[1] Composite materials are at the best in their efficiency for several reasons. Their composition includes at least two species, each possessing two distinct properties.[2] By

[a]*Department of Chemistry, School of Science, University of Management and Technology, Lahore 54770, Pakistan*

[b]*Department of Chemical and Biological Engineering, Gachon University, Seongnam-13120, Republic of Korea. E-mail: Muhammadarif2861@yahoo.com; Muhammadarif@umt.edu.pk; toheed@gachon.ac.kr*

Muhammad Arif

Dr Muhammad Arif has been Professor (Assistant) of Chemistry in the Department of Chemistry, University of Management and Technology, Lahore, since 2022. He has been working as lecturer in Chemistry in the Department of Chemistry, School of Science, University of Management and Technology, Lahore from 2017 to 2022. He has completed his PhD in Chemistry from the University of the Punjab, Lahore, Pakistan. He obtained his MPhil in Chemistry and MSc in Organic Chemistry degrees from Quaid-i-Azam University Islamabad, Islamabad, and Institute of Chemistry, University of the Punjab, Lahore, Pakistan, respectively. His research area is synthesis, characterization and applications of metal nanoparticles fabricated in microgels and ligands.

Toheed Akhter

Dr Toheed Akhter, PhD, is Assistant Professor at Gachon University, South Korea, specializing in polymer and porous materials. He completed his PhD jointly from KIAST, South Korea, and Quaid-i-Azam University, Pakistan. Dr Akhter has held postdoctoral positions at KAIST and UNIST, South Korea, and previously served as Assistant and Associate Professor at UMT, Pakistan. His research focuses on synthesizing and characterizing innovative materials for diverse applications.

altering the nature and quantity of these constituents, the resulting composite material properties can be finely tuned, which exhibit unique characteristics.[3,4] In nanomaterial–polymer composites, this tuning property mainly depends on the structure of organic polymers.[5–8] Crosslinked organic polymers are the best with respect to this tuning property.[9,10] The crosslinked network of organic polymers exhibits swelling and deswelling behaviors under stimulus conditions such as temperature,[11] pH,[12] and ionic strength.[13] The crosslinked network of organic polymers that show stimuli–responsive behavior is called a smart polymer.[14–20] The best performance of these smart organic polymer-based composites with respect to specific applications can be achieved by adjusting stimulus conditions.[21–25] Furthermore, nanomaterials have influence on the potential of composites.[26,27] Recent advancements in nanoscience have focused on leveraging the remarkable properties of nanofillers. Nanomaterials show excellent efficiency owing to their high surface-to-volume ratios[28] and quantum effects established at sub-micron scales.[29] Among the composite materials, polymer matrix composites are the most prevalent owing to their low density,[29] low cost,[30] and ease of use.[31] Nanomaterial–polymer composites have significant applications in biomedical,[32,33] environmental,[34,35] and engineering[36] fields.

Nanomaterials show exceptional hardness and remarkable stiffness, which make them valuable as reinforcing agents in polymer matrices.[37,38] Minor additions of nanomaterials (approximately 1 wt%) can significantly enhance the mechanical properties of polymers by up to 100% owing to their high efficiency. This enhancement is commonly attributed to the high surface area of nanomaterials, facilitating interactions that contribute to the developed properties.

Inorganic[39] or organic[40] substances are used as fillers and reinforcement in polymeric systems. Various nanomaterials are employed to enhance the properties of polymer matrixes such as carbon allotropes (including carbon dots,[41] graphene oxide,[42] carbon nanotubes,[43] and carbon fibers[44]), ceramics (TiO_2,[45] ZnO,[46] Fe_3O_4,[47] CeO_2,[37] SiO_2,[24] and TiO_2/carbon nanotubes[5]), and metals (such as Au/Ag,[12] Au,[48] Pt,[49] Pd,[50] Ag,[51] and Fe (ref. 52)). Among these nanomaterials, ceramic nanomaterials have gained significant interest due to their ready accessibility, and simple synthetic approaches.[53] The integration of ceramic nanoparticles into the polymeric network of organic polymers not only significantly enhances mechanical and thermal stability but also introduces novel functionalities depending on the structure,[54] chemical composition,[55] and size[56] of these ceramic nanofillers.

TiO_2 is more important than other ceramic nanoparticles due to its low-cost composites,[57] high performance for adsorption[58] as well as photocatalytic degradation,[59] comparatively small particle size,[60] ease of handling,[61] tunable properties,[62] high surface area,[63] and non-toxic nature.[64] TiO_2 nanoparticles also have importance due to their hydrophilicity,[65] chemical stability,[66] widespread availability,[67] and a range of other beneficial properties.[68–70] The surface chemistry of nanomaterials is commonly modified with reinforcing agents to establish strong interactions between polymer matrices and nanofillers in TiO_2–polymer composites (TPCs).[71–73] Various approaches can be employed to modify the surface properties of TiO_2 such as (i) inducing the coordination of small molecules through chemisorption, facilitated by proton transfer *via* hydrogen bond formation,[74] (ii) surface alteration *via* the presence of hydroxyl reactive groups and adsorbed species on TiO_2, leading to surface modification through the formation of covalent bonds with certain coupling agents,[75] (iii) using grafting techniques of monomers and comonomers in the form of polymers on the TiO_2 surface to generate electrostatic forces of attraction.[76]

TiO_2 nanoparticles are used in various fields including solar cells,[77] sensors,[78] optical devices,[79] and water purification membranes.[80] Leveraging the adaptable properties of TiO_2 nanoparticles, TiO_2–polymer composites have been developed for diverse applications,[81–84] which exhibit more efficiency than TiO_2 alone. These crosslinked organic polymers along with TiO_2 particles have even more importance than TiO_2 particles alone because TiO_2–polymer composites have both TiO_2 particles and crosslinked organic properties. In addition, the use of nano-TiO_2 (which effectively absorbs and reflects ultraviolet rays) enhances the high-temperature performance and aging resistance of polymer composites, to modify polymer-modified composites.[85–87] Consequently, these engineered TiO_2–polymer composites offer versatility for various purposes. To the best of our knowledge, various articles are reported on TiO_2 particles[88–90] and crosslinked organic polymers[91–93] separately, but a review on TiO_2 particles decorated in crosslinked organic polymers has not yet been reported. The aim of this review article is to provide complete details of the synthesis, classifications, characterizations, and applications of TiO_2 particles in crosslinked organic polymers. Additionally, it provides information on the factors that enhance their performance in different fields such as adsorption and photocatalysis.

2. Classifications

The TiO_2–polymer composites (TPCs) with a crosslinked network can be divided into various classes on the basis of (i) crosslinking nature and (ii) morphologies of composites. Explanations related to these classes are given below.

2.1. Classifications on the basis of crosslinking nature

The crosslinked structure of TPC can be formed using different crosslinkers. These crosslinkers can be (i) metal cations, (ii) organic molecules and (iii) TiO_2 itself. Let us now discuss these classes one by one.

2.1.1. TiO_2 as a crosslinker. In this category, no external crosslinker is needed for the synthesis of TPC. In some cases, TiO_2 nanoparticles also act as crosslinkers to form crosslinked structures of TPC. The structure of TiO_2 has Ti–O–H bonds, which can make hydrogen bonding with the structure of organic polymers. This hydrogen bonding is responsible for the formation of a crosslinked network of TPCs. This crosslinked network of TPCs can be decreased by external stimuli such as temperature, radiation, pH, and the content of ionic salts. All

these factors directly affect the strength of hydrogen bonding present between Ti–O–H and organic polymers. For example, the pH of the medium has influence on the crosslinking strength. The zero electric point of TiO_2 is 6.8. If pH $\geq$ 6.8, the oxygen and hydrogen bonds of Ti–O–H are broken and the size of TPC increases from the normal value due to deprotonation and then electrostatic repulsion between Ti–O^- anions. Due to this conversion of the structure of TPC, hydrogen bonding also gets altered, usually it is decreased. Similarly, Ti–O–H shifts into Ti–O^+H_2 at pH $\leq$ 6.8. In this way, the crosslinking density of TPC varies with the pH of the medium.[75] Therefore, the performance of TPC is also affected due to this conversion. Similarly, kinetic energy also influences this hydrogen bonding as the kinetic energy of TPC varies. Therefore, their performance for applications is also affected with these stimulus-responsive behaviors. The structure of monomers is also affected on their potential of applications. For example, a poly(acrylic acid)–TiO_2 composite has two groups (–COOH, –O–H) in its structure, which can donate their protons.[94] One (–COOH) is from poly(acrylic acid) and the other (Ti–O–H) from TiO_2. Such systems are also in swelling state after the conversion of –COOH groups into $-COO^-$ ions and before the isoelectric point of TiO_2. This conversion increases the adsorption capacity (due to large surface area and available spaces) and photocatalytic performance (due to easy approach of reactant molecules on the surface of TiO_2) of TPC. In the swelling state, the reactant molecules easily reach the surface of TiO_2 and easily degrade. Therefore, the degradation rate increases with swelling. The porosity of TPC is very important with respect to adsorption and photocatalytic activity. This porosity of TPC can be controlled with the content of TiO_2. The area of pores decreases with the increase in the content of TiO_2 due to increase in the crosslinking density of TPC.[95]

The crosslinking structure of such TiO_2–polymer composites is not very stable and this crosslinking value changes with varying the conditions of medium. The loaded materials in these TPC are easily released due to decrease in the crosslinking density with external stimuli. Some amount of TiO_2 also comes out from TPC systems. The crosslinking density of such systems also decreased with centrifugation. Therefore, such systems are not easily recycled, and their performance rapidly decreases after recycling.

2.1.2. Crosslinking with covalent bond formation. The crosslinked network of TPCs can be formed by covalent bond formation with a suitable crosslinker such as methacrylic anhydride (MAAn),[96] ethylene-glycol-diacrylate (EGDA),[97] glutaraldehyde (GA)[98] and *N*,*N*′-methylene-bis-acrylamide (NMBA).[99] These types of TPCs are mostly reported in the literature with *N*,*N*′-methylene-bis-acrylamide[76,100,101] as crosslinkers due to their high stability. Such systems are used in various fields such as adsorption[102] and photocatalytic degradation[103] of pollutants, drug delivery,[104] and reduction of Cr(VI)[105] ions from water.

By crosslinking with covalent bond formation, the TPC has more advantages than the *aforementioned* classes due to high stability and reversible stimuli responsive behavior. These systems show reversible swelling and deswelling behaviors under different values of temperature[106] and pH (ref. 107) of the medium without deformation in their structures. These types of TPC can be easily recycled without losing their performance.[108] Such stability is not present in the above-discussed classes.

2.2. Morphological classification of TPCs

TPCs can be classified on the basis of morphology into various classes, as shown in Fig. 1. These classes are given below.

2.2.1. Homogenous microspheres. In homogenous microspheres, the TiO_2 nanoparticles are uniformly distributed into the crosslinked network of organic polymers, as shown in Fig. 1(a). The compositions in each part of the structure of such classes are uniform. Such types of TPCs are widely reported in the literature.[74,109] These systems exhibit swelling and deswelling properties under various stimuli conditions.[110,111] The sensitivity of these TPCs to stimuli significantly influences their capabilities in catalysis, drug delivery, and adsorption. Adsorption, photocatalysis, and drug delivery by these systems can be controlled by controlling the diffusion rate of reactant molecules from the bulk region to the surface of TiO_2 across the crosslinked network. Therefore, these systems have tunable properties, which can be adjusted according to the conditions.

The adsorption and drug delivery properties of these composites depend on the nature of crosslinked polymers. These polymers also exhibit selectivity towards adsorption and rejection of pollutants due to electrostatic attraction (in case of

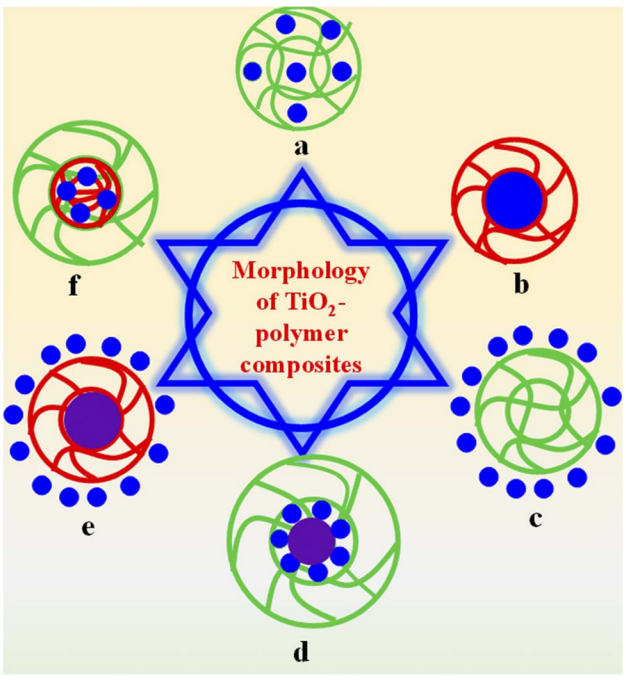

Fig. 1 Classifications of TPCs on the basis of morphology: (a) homogenous microspheres, (b) TiO_2 enclosed in crosslinked organic polymers, (c) crosslinked organic polymer enclosed in TiO_2 nanoparticles, (d) biomolecule enclosed in a layer of TiO_2 encapsulated in crosslinked polymers, (e) inorganic enclosed in crosslinked polymer encapsulated in TiO_2 nanoparticles and (f) TiO_2 nanoparticle-decorated crosslinked organic polymer enclosed in another crosslinked polymer.

opposite charges) and repulsion (in case of same charges).[112] These attractions also have effect on the loading and release of drugs. The main drawback of these composites is ultrafast-centrifugation, and some content of TiO_2 is leached out during this recycling process. Therefore, the catalytic efficiency of these composites decreases rapidly with the recycling process.

The tranquil nature of catalytic activity, adsorption capacity, and drug delivery in these systems stems from the effortless diffusion of reactive components. Enhanced stability arises from the encapsulation of silver nanoparticles within electron-donating groups. These hybrid microgels are categorized into two classes based on the presence of either one (monometallic) or two (bimetallic) metal nanoparticles within the microgels. Such systems are further classified into two classes: (a) TiO_2 nanoparticles decorated in crosslinked organic polymers and (b) TiO_2 and other metal oxide or metal sulfide nanoparticles decorated in crosslinked networks.

In TiO_2 nanoparticles decorated in the crosslinked network, no other type of metal oxide or sulfide nanoparticle is present in the structure of TPCs. Such systems are frequently reported in the literature. They have good performance with respect to adsorption, photocatalysis, and drug delivery, while the other classes (TiO_2 and other metal oxide or metal sulfide nanoparticles decorated in crosslinked networks) have more advantages than the aforementioned classes due to the synergistic effect. The value of energy band gap in these composites further decreases. Therefore, the valence electrons can easily jump from the valence band to the conduction band, and the degradation efficiency increases in the presence of photons.[113] Similar effects of these composites are also present for other applications such as antibacterial activity.[114]

2.2.2. TiO_2 enclosed in crosslinked organic polymers. In crosslinked organic polymer-enclosed TiO_2, TiO_2 nanoparticles are trapped with crosslinked organic polymers to form a core–shell system, in which TiO_2 is present in the core region and crosslinked organic polymers in the shell, as shown in Fig. 1(b). Such classes are very rarely reported in the literature. These core–shell systems are effective for adsorption purposes, but their photocatalytic efficiency is very low. The photocatalytic activity of these systems is due to the presence of TiO_2. When TiO_2 is present in the core, then the approach of pollutant molecules to the surface of TiO_2 takes more time due to the longer distance between the pollutant present in the bulk region and the surface of TiO_2. The adsorption property of such systems does not have much effect on this position of TiO_2 because the crosslinked organic polymer region is a better region for the adsorption of pollutants than the TiO_2 region. The adsorption capacity of such core–shell systems is greater than TiO_2 lone due to more interaction with pollutants and loading drugs.[115] These systems can also be used for drug delivery due to the organic shell region.[116] The releasing of loaded drug can be controlled with the stability of the organic shell. The stability of these core–shell systems decreases with time (in days). Therefore, the loaded drugs are also released rapidly from the core–shell systems to the target place. This releasing efficiency can be controlled by controlling the stability of the core–shell systems. This releasing efficiency is controlled with the crosslinked structure. The crosslinked structure of organic polymers stabilized the shell region and also controlled the release of loaded drugs.[117]

2.2.3. Crosslinked organic polymer enclosed in TiO_2 nanoparticles. In the TiO_2 nanoparticle-enclosed crosslinked organic polymer, the crosslinked organic polymer is surrounded by TiO_2 nanoparticles to form core–shell systems, as shown in Fig. 1(c). In these core–shell systems, the crosslinked organic polymer is present in the core region and TiO_2 nanoparticles in the shell.[118] The formation of such types of core–shell systems depends upon the size of TiO_2 nanoparticles and the crosslinking density of organic polymers. If the size of TiO_2 nanoparticles is large or the crosslinking density of organic polymer is high or both, then the TiO_2 nanoparticles cannot come into the sieves of crosslinked organic polymer and adsorb onto the surface of the organic polymer due to electrostatic interactions.[119] Such systems have a better photocatalytic activity than that of crosslinked organic polymer-enclosed TiO_2 systems and homogenous microspheres. The pollutants can easily reach the surface of TiO_2 (main photocatalyst) than other systems. Therefore, the photocatalytic degradation rate of such core–shell systems is greater than the aforementioned systems. Because the pollutant takes more time to reach the surface of TiO_2 nanoparticles through the crosslinked network in other systems, while the pollutants reach the TiO_2 surface directly in these systems. Their photocatalytic activity is further enhanced with the increase in the content of TiO_2 nanoparticles in these core–shell systems. The activity sites of such core–shell systems increase with the increase in the content of TiO_2 nanoparticles. Therefore, their activity increased with the TiO_2 content.[120] The adsorption capacity of such systems is lesser than that of other systems due to the less adsorption capacity of TiO_2 nanoparticles than that of the crosslinked network of organic polymers. However, the percentage removal of these systems is higher than that of others due to both adsorption and photocatalytic properties.[121]

These systems are not reported for drug delivery. Their antibacterial activity and drug delivery performance are the available fields for research. These systems can be used for the fabrication of clothes due to their antibacterial activity, and protection from UV radiation. These properties become more suitable in synergistic effects.[24] More research is needed on these systems due to their effective performance in various fields.

2.2.4. Biomolecule enclosed in a layer of TiO_2 encapsulated in crosslinked polymers. In these systems, the core is made with biomolecules alone or with other species, which is surrounded with a layer of TiO_2 nanoparticles, which is further surrounded by a crosslinked polymer to form core-layer–shell systems, as shown in Fig. 1(d). The adsorption capacity of such systems is greater than that of the core enclosed in a layer. Such systems are very suitable for adsorption processes due to polar crosslinked shell networks. These polar crosslinked networks absorb more contents of pollutants. The TiO_2 layer then facilitates these systems to degrade the adsorbed pollutants due to the photocatalytic effect.[122] The photocatalytic effects of these

systems are less than that of homogenous microspheres and organic polymer enclosed in TiO_2 due to consumption of time during the approach of pollutants from the bulk region to the TiO_2 surface. They also show catalytic degradation behavior of pollutants from water under sonication. The power of sonication also promotes the electrons of valence band to the conduction band of TiO_2 nanoparticles. Therefore, such hybrid systems can show catalytic activity in sonication to degrade pollutants.[13]

Biomolecules enclosed in a layer of TiO_2 encapsulated in crosslinked polymer systems cannot lose TiO_2 nanoparticles from their structure during recycling. Such systems can also be used for drug delivery due to the stimulus–responsive behavior, polarity and porosity of the shell region. The porosity of such systems effect of loading of drug, while polarity on loading and releasing of drug from these systems. Such systems are not applied for this purpose yet. This is an empty space for research in these systems. They are also not used for antibacterial and other applications. New researchers can work in these fields by these types of systems.

2.2.5. Inorganic enclosed in crosslinked polymer encapsulated in TiO_2 nanoparticles. In these systems, inorganic particles (SiO_2 or Fe_2O_3 or Fe_3O_4) are present as core which is surrounded by the crosslinked polymer shell which is further encapsulated with TiO_2 nanoparticles as shown in Fig. 1(e). Such systems are very rarely reported in the literature. These systems have a higher photocatalytic activity than that of other aforementioned systems (except crosslinked polymer enclosed in TiO_2) because the pollutants can directly come into contact with the photocatalytic material (TiO_2 nanoparticles). These systems are also useful for the adsorption of pollutants due to Ti–O–H bonds. These polar bonds can make hydrogen bonding with polar pollutants, and therefore, the pollutants adsorbed onto the surface of these systems.[123] The adsorption property of such systems can be changed by changing the environment of medium such as pH, temperature, contact time, dose of adsorbent, and concentration of pollutants. These parameters affect the interactions present between the pollutants and the adsorbents.

These systems are not used for photocatalytic degradation of pollutants, drug delivery, and antibacterial applications. Their adsorption study was also conducted different types of pollutants. These systems are very useful to those researchers working on photocatalysis. These systems can easily be recycled due to their large density (due to solid inorganic core). However, leakage of TiO_2 nanoparticles from these systems during recycling is the only drawback of these systems, which can be controlled by using magnetic nanoparticles (Fe_3O_4 or Fe_2O_3) as inorganic cores.

2.2.6. TiO_2 nanoparticle-decorated crosslinked organic polymer enclosed in another crosslinked polymer. In these systems, TiO_2 nanoparticles are decorated in crosslinked organic polymers which are then further encapsulated with another crosslinked polymer network, as shown in Fig. 1(f). Such systems are also rarely reported in the literature. In such systems, the crosslinked network of the shell region is responsible for the adsorption property and stimulus-responsive behavior. The pollutants come into the crosslinked network of the shell region from the bulk region due to electrostatic interactions. The photocatalytic activity of such systems is very low due to slow approach and less content approach of pollutants to the surface of TiO_2. This approach depends on the flow of water molecules from the outer region to the hybrid systems and from hybrid systems to the outer region of the medium. Therefore, those systems which can uptake more water molecules should be more efficient photocatalysts than those in which the water intake is very low. Those systems which absorb more water molecules have a high value of hydrodynamic diameter, and the area of pores is very high. Therefore, water molecules can easily enter into the network and out of the network.[39] Similarly, the pollutant can easily enter into the network along with water molecules in swelling hybrid systems and reach the surface of TiO_2 nanoparticles. These nanoparticles degraded these pollutant molecules into CO_2 and water molecules.[43]

3. Synthesis

TiO_2–polymer composites can be synthesized by different methods. These methods are given below.

3.1. Simultaneous mixing of TiO_2 nanoparticles and monomers, comonomers, and crosslinker to form TiO_2–polymer composites (TPCs)

In this method, all components are first mixed by sonication and stirring. The electrostatic forces take part to come close with each other. In this way, the solubility of all components increased in the medium. After that, a free radical initiator is added in to the mixture to start polymerization. The reason for mixing is that the composition of all components is homogenous at all places of medium. For instance, Zhou *et al.*[102] have reported the synthesis of TiO_2 nanoparticles decorated in chitosan-poly(*N*-isopropylacrylamide) TiO_2-CS-P(NIPAM) by a similar method, as shown in Fig. 2. They prepared a solution of chitosan in 1% acetic acid solution and then added into a three-necked round-bottomed flask containing deionized water along with *N*-isopropylacrylamide (NIPAM) (monomer), *N*,*N*′-methylenebisacrylamide (NMBA) (crosslinker), and TiO_2 nanoparticles and sonicated for 10 min. The mixture was purged with argon (Ar) for 30 min to remove oxygen. Ammonium-per-sulfate (AmPS) (free radical initiator) and *N*,*N*,*N*′,*N*′-tetramethylethylenediamine (NTMEDA) (accelerator) were then added into the above mixture under vigorous stirring at 20 °C for 1 h. Xu *et al.*[111] and You *et al.*[107] have also reported the synthesis of TiO_2–polymer composites by similar methods.

In this method, homogenous microspheres of composites were formed. Therefore, it is not suitable for core–shell systems of composites. This method is very simple and easy to perform, but the size control of TiO_2 and microgels is a challenge in this method. The size of TiO_2 and crosslinked polymer network is very important with respect to their applications. Therefore, this method is not suitable for those researchers, which require specific sized TiO_2–polymer composites.

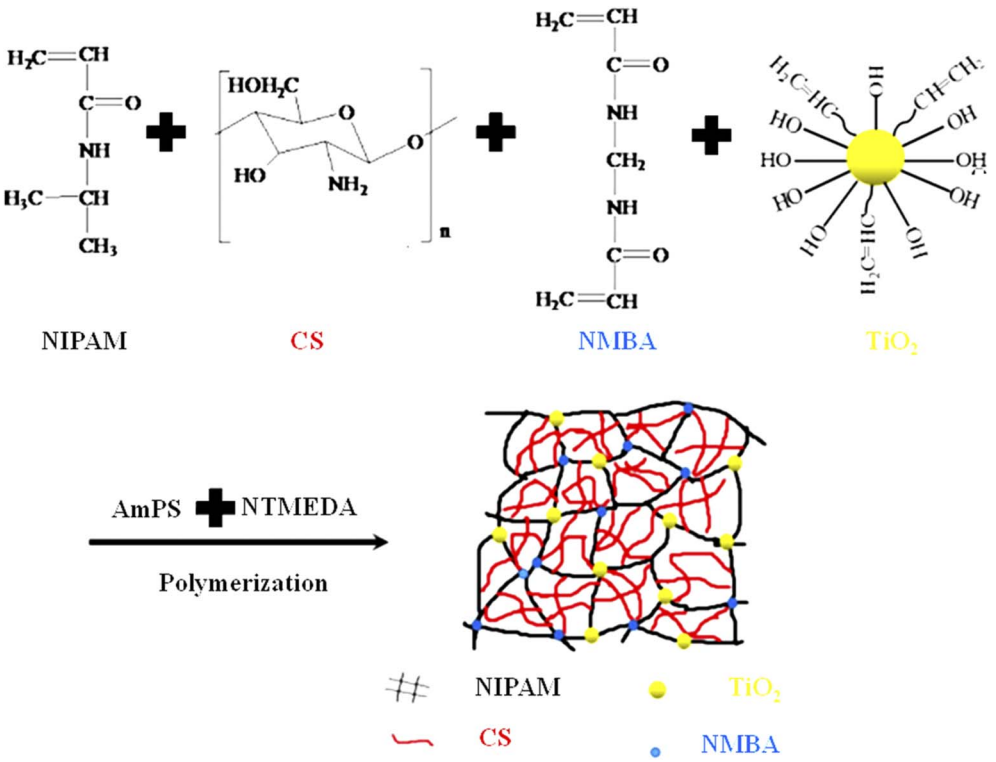

Fig. 2 Synthesis of TiO_2 nanoparticles decorated in chitosan-poly(*N*-isopropylacrylamide) TiO_2-CS-P(NIPAM) by simultaneously mixing all components (reproduced from ref. 102 with permission from Elsevier, copyright 2017).[102]

3.2. Insertion of TiO_2 nanoparticles in crosslinker polymer microgels

In this method, both crosslinked organic polymers and TiO_2 were synthesized separately. The microgels have polar parts in their structure, which interact with the TiO_2 particles. Due to this interaction, the TiO_2 particles are moved towards the microgel network from the medium. The diffusion of TiO_2 nanoparticles depends on the size of TiO_2 and the crosslinking density. More particles are moved inside if the size of the particles is small with low crosslinking density. In the low crosslinking density, the area of sieves of crosslinked network is large. Therefore, the TiO_2 particles easily diffuse into the network of microgels. The density of crosslinking networks can be controlled by the swelling/deswelling behavior in smart microgel composites. The insertion of TiO_2 has rapidly occurred in the swelling state of microgels. In this state (swelling state), the surface area of pores is maximum and TiO_2 can easily diffuse into the crosslinked network of microgels along with water molecules and *vice versa*. Škorić *et al.*[121] synthesised TiO_2 nanoparticles decorated in chitosan-poly(methacrylic acid) TiO_2-CS-P(MAAc), as shown in Fig. 3. They synthesized the first TiO_2 nanoparticles by using $TiCl_4$. The solution of $TiCl_4$ was cooled till −20 °C and then added in another beaker containing deionized water at 4 °C under vigorous stirring. The stirring continued for further 30 min at that temperature. The pH of the solution was in the range of 0–1 (depending on content of $TiCl_4$). The solution was dialyzed to pH = 3.5. For the synthesis of microgels, chitosan (comonomer), methacrylic acid (monomer) and *N*,*N*′-methylenebisacrylamide (NMBA) (crosslinker) were added into a three-necked flask containing deionized water. The mixture was stirred until a homogenous mixture was obtained and heated at 50 °C. Then potassium-per-sulfate (PoPS) (free radical initiator) was added dropwise into the mixture under nitrogen purging and stirring (450 rpm, $T = 50$ °C). After 15 min, *N*,*N*,*N*′,*N*′-tetramethylethylenediamine (NTMEDA) (accelerator) was also added into the mixture and the reaction was proceeded for further 3 h. The product was purified with petroleum ether and deionized water respectively and dried at 37 °C. To synthesize the composite, the synthesized microgel was first swelled for 2 h and then TiO_2 nanoparticles were mixed with vigorous stirring (Yun *et al.*[103] and Galata *et al.*).[119] A similar synthetic method was reported by Kazemi *et al.*[124] and Zazakowny.[60]

This method is also easy to synthesise TiO_2–polymer composites. This method is applicable only for homogenous composite microspheres and microgels covered with TiO_2 nanoparticles. TiO_2 nanoparticles enclosed in microgel composites cannot be synthesized by this method. This method requires more time during synthesis. During insertion of TiO_2 nanoparticles, the pore size of microgels and size of TiO_2 nanoparticles are the most important parameters. If the size of TiO_2 nanoparticles is greater than the pore size of microgels, then TiO_2 nanoparticles cannot come into the sieves of microgels and adsorb onto the surface of microgels only. Insertion is possible if the size of TiO_2 is smaller than the pore size of microgels. Therefore, controlling the size is the main key point for this method.

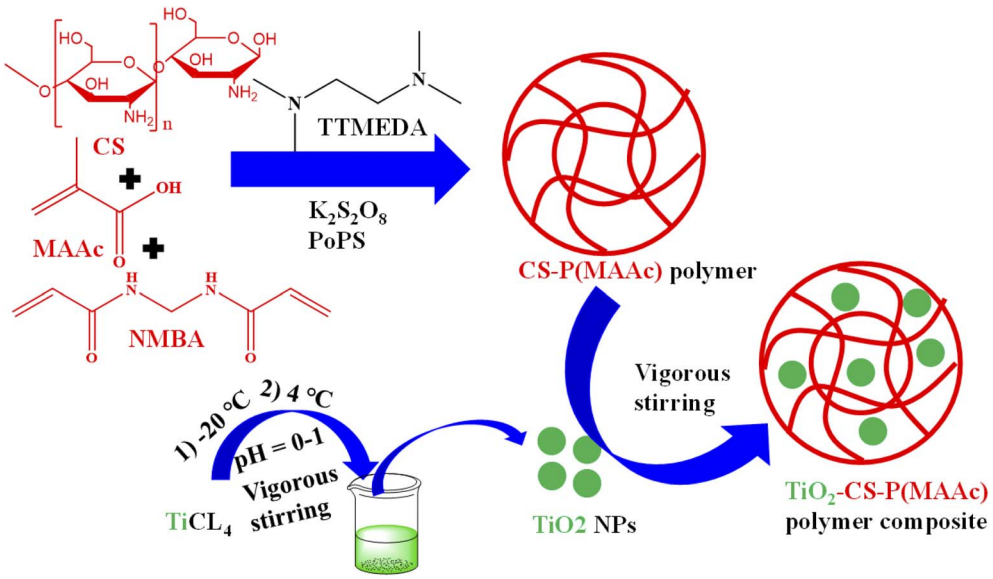

Fig. 3 Synthesis of chitosan-poly(methacrylic acid) CS-P(MAAc) followed by TiO_2 to form TiO_2-CS-P(MAAc).

3.3. Simultaneous mixing of monomers, comonomers with TiO_2 nanoparticles followed by crosslinkers (without free radical initiators)

In this method, the polar monomers are mixed with TiO_2 in an acidic medium. A bond is generated between the oxygen of TiO_2 with polar functional (–COOH, –OH, and $–NH_2$) groups of monomers. After that, a crosslinker was added to form a crosslinked network containing composites. Homogeneous composites of organic polymers with TiO_2 were synthesized by this method. Maximum loading of TiO_2 nanoparticles occurs in this method. Therefore, the photocatalytic activity of such synthesized composites is greater than the composites synthesized by the aforementioned methods. Mohammad *et al.*[125] synthesized TiO_2 nanoparticles decorated in the crosslinked network of chitosan–glyoxal (CS–GX), as shown in Fig. 4. They mixed TiO_2 nanoparticles and chitosan and then stirred in 5% acetic acid for 24 h under vigorous stirring. This mixture was then added into a basic medium at a drop rate of 1 mL min^{-1}. The mixture was then heated at 40 °C after adding glyoxal (GX) (crosslinker). The product was washed extensively to remove the impurities. A similar method was reported by Liu *et al.*[105]

This TiO_2–polymer composite synthetic method does not waste the amount of TiO_2 nanoparticles during synthesis but some content of TiO_2 is lost during other synthetic methods due to hydrogen bonding of TiO_2 with water molecules while intra molecular hydrogen bonding in the crosslinked network of organic polymers. The synthesis of monodispersed TiO_2 nanoparticles is not possible in this synthetic method. This synthetic method is applicable only for homogenous hybrid microgels.

3.4. Synthesis of TiO_2–polymer composites without free radicals

In this method, the crosslinked network system is synthesized without any external free radical initiator. In this method, radicals are generated by thermal decomposition of pi bonds due to their weakness. The Pi bond is a weak bond as compared to sima bond owing to parallel overlapping. Therefore, this bond can easily break with the generation of free radicals to produce a crosslinked network of conditions. The radicals are generated by applying thermal radiations[126] and photons[97] on the monomers. These energies converted the monomers into radicals. The monomers or commoners act as self-crosslinkers during the synthesis. Wei *et al.*[127] have synthesized TiO_2 decorated in poly(ethylene glycol diacrylate) TiO_2-P(EGDA) with UV irradiation. They mixed the photo-initiator and ethylene glycol diacrylate (EGDA) in ethanol with vigorous stirring for 30 min. Then TiO_2 nanoparticles were dispersed in an aqueous medium and ultra-sonicated for 30 min to remove dissolved oxygen. Then this dispersion along with P(EGDA) is spread in a chamber along with a plastic injector. The radiations of UV-LED lamp (240 mw cm^{-2}) fell on this mixture for 700 ms to form composites. Then the product was treated with plasma for 30 s. The product was then treated by ultra-sound in ethanol and water to remove impurities. Wu *et al.*[128] have also been reported the synthesis of TiO_2 nanoparticles in graphene oxide-poly(*N,N′*-dimethylacrylamide) TiO_2-GO-P(NDMAAm) systems. They mixed graphene oxide (GO), *N,N′*-dimethylacrylamide (NDMAAm), NMBA, and TiO_2 in an aqueous medium. UV light (for 5 min) or sun light (for 30 min) irradiated on this mixture to form a brown elastic product. The irradiation continued for a further 1 h to change the light brown color into dark brown. This color variation indicated the conversion of graphene oxide into reduced graphene. Kandel *et al.*[115] have also reported the synthesis of TiO_2–polymer composites by an electro-copolymerization method (without free radical initiator).

Homogenous composites are formed in this approach. This synthetic method is very simple and easy to use but the control of size of both TiO_2 nanoparticles and crosslinked polymers is not controllable. Complete polymerization and proper orientation of

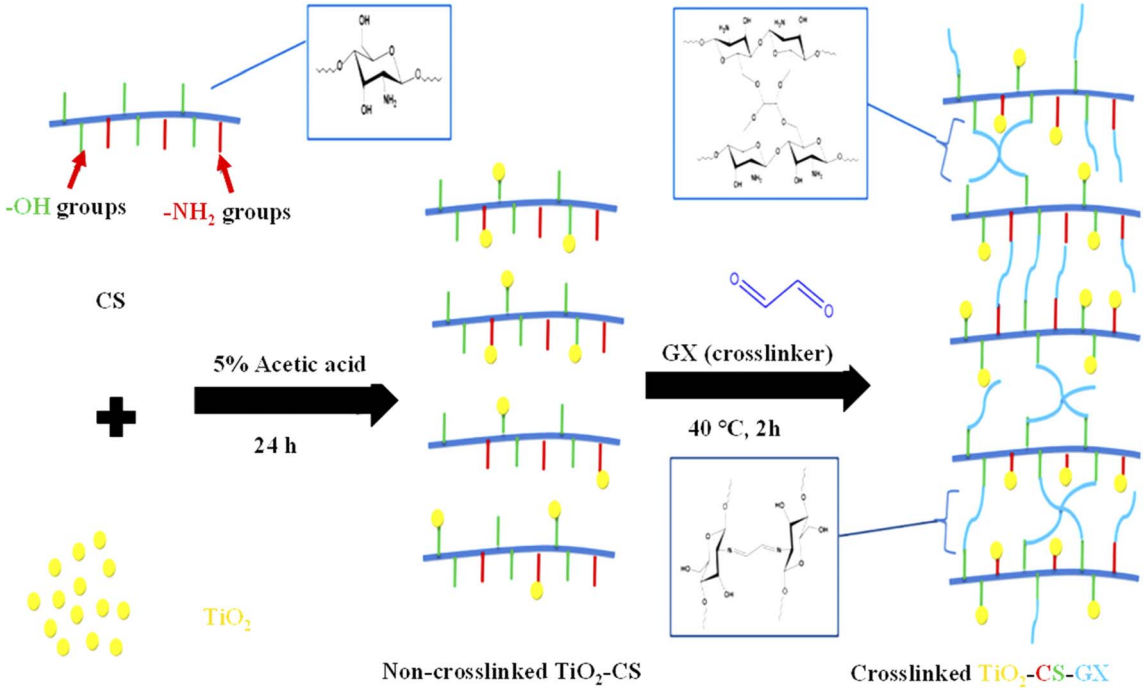

Fig. 4 Synthesis of TiO_2–CS–GX by simultaneously mixing TiO_2, CS followed by GX crosslinkers (reproduced from ref. 125 with permission from Elsevier, copyright 2019).[125]

polymerization methods is very important which cannot be controlled in this method. The value of radiation is not homogenous for all monomers. Therefore, monodisperse TiO_2–polymer composites are not properly synthesized by this method.

4. Characterizations

Various techniques are employed to analyze the structure, size, morphology, and composition of TiO_2 nanoparticles decorated within organic polymers, as listed in Table 1. These techniques serve to differentiate the structural morphology, porosity, and stimuli behavior of TiO_2 nanoparticles in polymer and polymer networks (without TiO_2). Specific characterization techniques include X-ray diffraction (XRD), dynamic light scattering (DLS), scanning electron microscopy (SEM),[129] energy-dispersive X-ray spectroscopy (EDX), high-resolution transmission electron microscopy (HR-TEM), wide-angle X-ray scattering (WAXS), ^{1}H-nuclear magnetic resonance spectroscopy (NMR), photoluminescence spectroscopy (PL), Raman spectroscopy (RS), transmission electron microscopy (TEM), UV-visible spectroscopy (UV-vis), laser light scattering spectrometry (LLS), photo correlation spectroscopy (PSC), attenuated total reflectance spectroscopy (ATR), differential mechanical analysis (DMA), differential scanning calorimetry (DSC), inductively coupled plasma atomic emission spectroscopy (ICP-AES), atomic force microscopy (AFM), polarizing optical microscopy (POM), inductively coupled plasma mass spectrometry (ICP-MS), Fourier transform infrared (FTIR) spectroscopy, inductively coupled plasma-optical emission spectrometry (ICP-OES), Brunauer Emmett Teller (BET) analysis,[131] and field emission scanning electron microscopy (FE-SEM).[140]

Advanced microscopic instruments such as TEM, AFM, HR-TEM, FE-SEM (ref. 140) and SEM are used to analyze the organic polymers with and without TiO_2 nanoparticles, aiming to explore their physical attributes. HR-TEM and TEM (ref. 46) are employed to examine the size, size distribution, and morphology of both the organic polymers with and without TiO_2. They are also used to investigate the dimensions, and shapes of both polymer microgels with and without TiO_2. Furthermore, AFM, SEM (as shown in Fig. 5(D–G)), and HR-TEM are used to investigate the surface morphology of organic polymers with and without TiO_2 present due to their structural arrangements, as shown in Fig. 5(H–K).

NMR, FTIR (as shown in Fig. 5(A)), and RS techniques are extensively employed to investigate the functionalities of resulting organic polymers and to differentiate the interactions within the polymeric network of organic polymers with and without TiO_2 nanoparticles. EDX and XRD (ref. 132) techniques serve to validate the presence and characteristics of TiO_2 nanoparticles within crosslinked polymeric networks. The crystalline structure of polymers with and without TiO_2 nanoparticles is assessed by XRD, as shown in Fig. 5(B). WAXS, Particle Size Analyzer, and DLS are used to measure the diameter range, size distribution and size of both crosslinked polymers and hybrid systems. UV/Vis/NIR spectroscopy is utilized to ascertain the volume phase transition temperature (VPTT) of crosslinked organic polymers with and without TiO_2 by measuring turbidity.

TGA,[133] DMA, and DSC (ref. 135) techniques are used to examine the thermal stability and decomposition characteristics of both organic polymers and their hybrid systems. TGA is also used to quantify the content of TiO_2 nanoparticles within organic polymers, as shown in Fig. 5(C). DLS/Photon correlation

Table 1 TiO_2–polymer composites with monomers and comonomers, applications, and characterization techniques

System	Structural morphology	Monomers and comonomers	Applications	Characterization techniques	References
TiO_2-SoA-P(Q-10)	Homogenous microsphere	SoA, Q-10	Antibacterial	SEM, *zeta potential*, DLS, UV-vis, TGA, *digital camera*	129
TiO_2-P(AAm-DMAAm)	Homogenous microsphere	AAm, DAAm	Photocatalytic activity	TEM, FTIR, UV-vis, SEM	130
TiO_2-P(AAm)	Homogenous microsphere	AAm	—	EDX, FTIR, TGA, XRD, BET	131
TiO_2–GG–P(AAm)	Homogenous microsphere	GG, AAm	Adsorption	FTIR, SEM, TGA, BET, TEM, EDS	132
TiO_2-P(VA)-C	Homogenous microsphere	VA, C	Conductance, water adsorption	TGA, XRD, UTM, SEM	133
TiO_2@CS, TiO_2–CeO_2@CS, CeO_2@CS	Core–shell	CS	Tissue engineering and water adsorption	SEM, XRD, UV-vis, *Fluorescence*, *Rheometer*, MTTS	37
TiO_2-PT-P(EOAAm), MgO-PT-P(EOAAm), CaO-PT-P(EOAAm), ZnO-PT-P(EOAAm)	Homogenous microsphere	PT, EOAAm	Antibacterial	FTIR, TEM, XRD, SEM	134
TiO_2-KCG-XG-GeG	Homogenous microsphere	KCG, GeG, XG	Antibacterial	FTIR, SEM, XRD, DSC, TGA, CA analyzer, UV-vis	135
TiO_2-P(VA), Fe_3O_2-P(VA)	Homogenous microsphere	VA	Biomass immobilization and wastewater treatment	SEM, FTIR, MTS, *Rheometer*	136
TiO_2-P(NIPAM-AAc)	Homogenous microsphere	NIPAM, AAc	—	TEM, DLS, *Zeta-sizer*, *Turbidometer*, UV-vis	137
TiO_2-P(VA)	Homogenous microsphere	VA	—	ESR, XRD, UV-vis	138
TiO_2-P(AAc-VP)	Homogenous microsphere	AAc, VP	Water uptake	DSC, TGA, SEM, EDX, FTIR	139
TiO_2-CMCS-P(VA)	Homogenous microsphere	CMCS, VA	Antibacterial	XRD, TGA, FE-SEM, SEM, *fluorescence,* FTIR	140
TiO_2-(AAm), TiO_2-(AAm-PoA)	Homogenous microsphere	AAm, PoA	Photocatalysis	BET, TEM, XRD, *particle-size analyzer*, UV-Vis	141
TiO_2-P(AMPS)	Homogenous microsphere	AMPS	Photocatalysis	BET, SEM, XRD, FTIR, TGA, UV-vis	142
TiO_2-P(VA)-P(AAc)	Homogenous microsphere	VA, AAc	Photocatalysis	SEM, FE-SEM, XRD, UV-vis	143
TiO_2-SoA-HPMC	Homogenous microsphere	SoA, HPMC	Drug delivery, anti-cancer	FTIR, SEM, DSC, XRD, TGA, DSC	83
TiO_2-CS	Homogenous microsphere	CS	Adsorption and antibacterial	FE-SEM, SEM, EDS, BET, FTIR, TGA	144
TiO_2/ZnO–P(HEMA-AMPS)	Homogenous microsphere	HEMA, AMPS	Adsorption	ATR-FTIR, EDS, SEM, XRD, HR-TEM, UV-vis	46
TiO_2-CS-P(AAm-IA), SiO_2-CS-P(AAm-IA)	Homogenous microsphere	CS, AAm, IA	Adsorption, antibacterial	EDX, BET, SEM, TGA, FTIR, AAS	145

spectroscopy (PCS) is employed to ascertain the size distribution and hydrodynamic size of polymers with and without TiO_2 nanoparticles. WAXS is utilized to characterize the structure and uniformity of synthesized hydrogels, providing valuable information about the network topology, and ensuring consistency in their structures. Rheological measurements are carried out to understand the viscoelastic properties of hydrogels.

Investigations into drug release encompass evaluating the cytotoxic effects of organic polymers and hybrid systems through MTTS (ref. 37) assays. The amount of drug released is quantified using the HPLC technique, while the loading and release of the drug are monitored by confocal laser scanning microscopy (CLSM). Furthermore, ICP-MS, ICP-OES, and ICP-AES were employed to determine the presence of TiO_2 nanoparticles incorporated into polymers. Table 1 provides a summary of the microgels containing TiO_2 nanoparticles, the characterization techniques employed, and their respective applications. Some characterization techniques are given in Fig. 5, which are used for the characterization of both polymer and TiO_2–polymer composites.

5. Applications of TiO_2–polymer composites

TiO_2–polymer composites have various applications in various fields, as shown in Fig. 6. These applications are discussed one-by-one in this section.

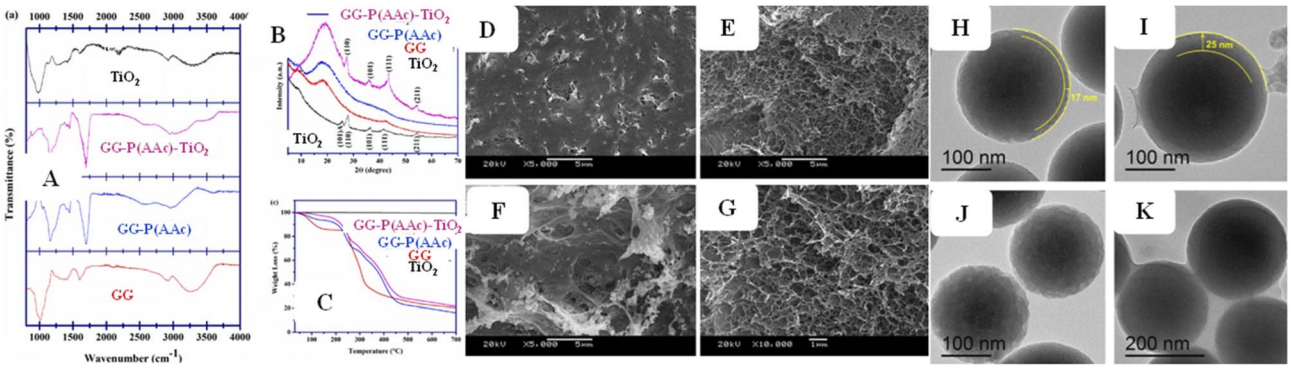

Fig. 5 Characterization techniques: (A) FTIR, (B) XRD and (C) TGA (reproduced from ref. 71 and 102 with permission from Elsevier, copyright 2022).[71,102] (D–G) SEM image (reproduced from ref. 74 with permission from Elsevier, copyright 2021).[74] (H–K) TEM image (reproduced from ref. 95 with permission from Elsevier, copyright 2019).[95]

5.1. Drug delivery

TiO_2–polymer composites can be used for drug delivery. The loading and releasing of drug from TiO_2–polymer composites depends upon the interactions present between the drug and the network of composites. The crosslinked network of polymers is made by the polymerization of monomers. Therefore, the interaction of network depends upon the nature of monomers used for the synthesis of crosslinked polymers.[104] The strength of interaction depends upon the nature of both the drug and the crosslinked polymeric network.[117] If the charge of the crosslinked network is opposite to the charges of drug, then maximum interactions are present between the drug and the composite. Therefore, maximum loading of drug occurs than other conditions of charges. Similarly, these interactions also affect the releasing behavior of drug.[110] Another reason of more and fewer loadings of drug is the swelling and deswelling nature

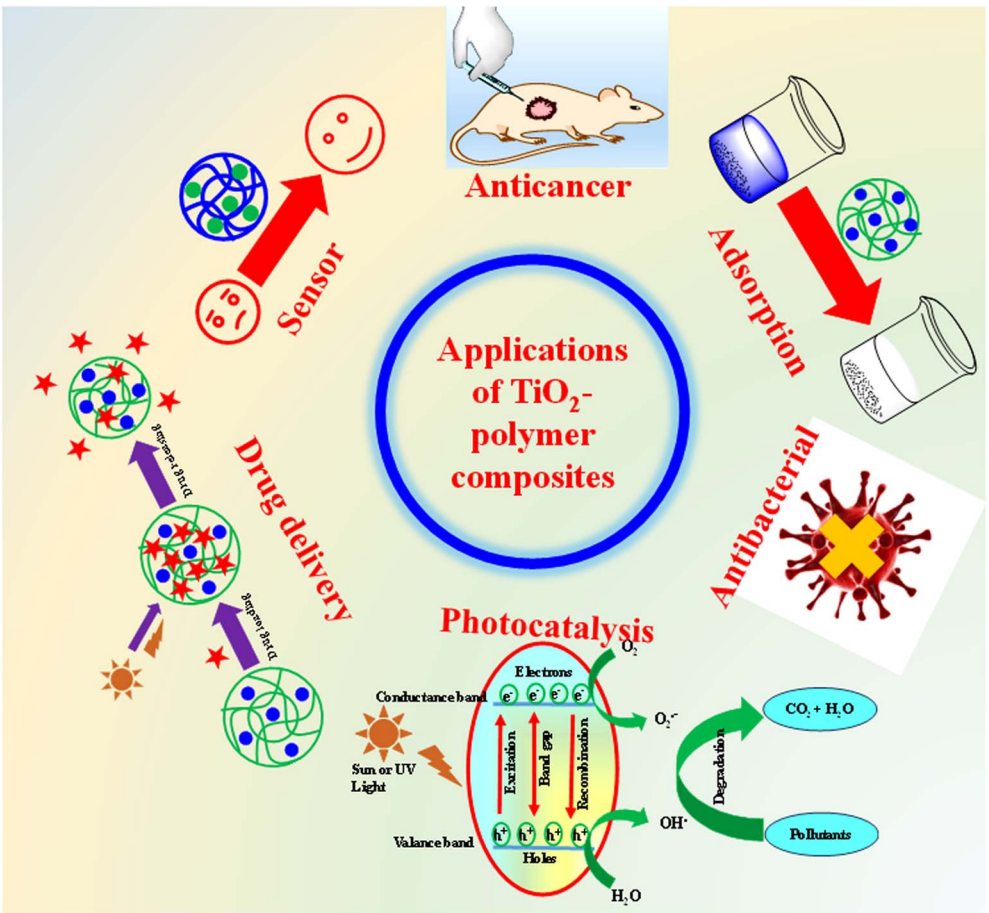

Fig. 6 Applications of TiO_2–polymer composites.

of polymers under stimulus conditions. Maximum loading of drug occurred in swelling state which is released after reaching the target place by the conversion of deswelling the state of hybrid systems, as shown in Fig. 7.[97]

During the swelling state, the drug comes into the sieves of crosslinked network along with water molecules due to electrostatic interactions. Interactions can be decreased by changing the conditions of environment. Therefore, the network is shifted from the swelling state to the deswelling state and the drug comes out from these sieves along with water molecules. This shifting of the swelling state into deswelling has occurred by changing the pH (ref. 73) and temperature[83] of the medium. Basically, there are two types of interactions: hydrophilic (interactions between water molecules and the structure of TiO_2–polymer composites) and hydrophobic (interactions present between different parts TiO_2–polymer composites). The strength of these interactions can be changed by changing the environment. The environment of TiO_2–polymer composites can be altered by varying the pH of the medium, temperature, and ionic strength. Therefore, these parameters also affect the loading and release of drugs from the network of composites. Therefore, the release and loading of drugs is controlled by these parameters. For example, the network of composites is present in the swelling state at low temperatures due to stronger hydrophilic interactions than hydrophobic interactions. While at high temperatures, the hydrophobic interactions dominate over the hydrophilic interactions. Therefore, water molecules come out and the composites shift from the swelling state to the deswelling state. Similarly, the pH of the medium also affects the swelling and deswelling behavior. Under these conditions, the phenomenon of protonation and deprotonation occurs in the structure of composites. Swelling occurs if the same charge is present in the structure of composites (due to electrostatic repulsion). Acidic composites show swelling behavior under basic conditions, while basic composites show swelling behavior under acidic conditions due to same charges under both conditions. Greater loading of drugs in composites also releases more amounts of drugs during the release process. In this way, the composites can be made more efficient for drug delivery by optimizing the conditions.

5.2. Anticancer

TiO_2–polymer composites exhibit potential in cancer treatment due to the delivery of anticancer drug. The incorporation of an anti-cancer drug into these TiO_2–polymer composites allows controlled release upon targeted radiation application. This release mechanism is facilitated by the deswelling behavior of TiO_2–polymer composites.[146] Some thionyl bonds of DNA also break due to the oxidation–reduction reactions, which occur by the presence of TiO_2 nanoparticles. The anti-cancer property of composites is even more in doped TiO_2–polymer composites due to the decrease in the energy band gap (doped materials prevent the combination of electron and hole pairs).[119] Therefore, composites provide an environment as a carrier for drug delivery as well as breaking the bonds of DNA molecules. The loaded drug is released at the target place by changing the temperature[52] or pH (ref. 146) of the medium. These conditions control the swelling and deswelling behavior of composites. The release of anticancer drug is very important factor for treatment. Some amounts of drug can be spread over some healthy cells during rapid release and destroy them. Therefore, control releasing is a suitable condition for cancer treatment.

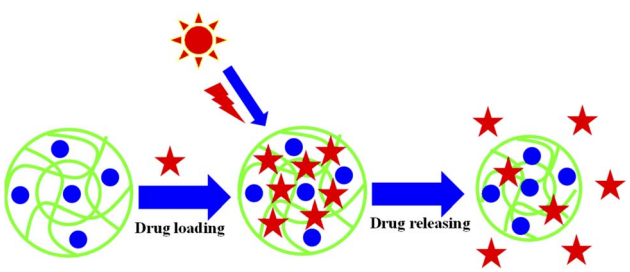

Fig. 7 Loading and release of drugs from TPC.

5.3. Antibacterial

Bacteria are the main source of diseases. Therefore, their killing is an essential condition for a healthy life. These bacteria are present everywhere. Therefore, they can easily enter our bodies and spread diseases. Different types of antibacterial agents can be used for their killing but the TiO_2–polymer composite is very efficient and eco-friendly in nature. They kill different types of bacteria such as *Escherichia coli* (*E. coli*),[72] *Staphylococcus aureus* (*S. aureus*),[147] *Candida albicans* (*C. albicans*),[134] and *Pseudomonas aeruginosa* (*P. aeruginosa*)[25] from body.

TiO_2–polymer composites exhibit efficient antibacterial activity. This antibacterial activity is mostly due to TiO_2 particles.[144] TiO_2 nanoparticles have a low energy band. The electrons of TiO_2 can easily jump from the valence band to the conduction band. In this way, TiO_2 can facilitate the occurrence of oxidation–reduction reactions. These oxidation–reduction reactions kill the bacteria. The oxidation–reduction reactions of TiO_2–polymer composite with the surface of bacteria depend upon TiO_2 particles. Therefore, antibacterial activity of composites depends upon the content of TiO_2 nanoparticles[135] in composites and the approach of bacteria to the surface of TiO_2 nanoparticles. Therefore, antibacterial activity of composites can be controlled by stimuli conditions as well as increasing the rate of jumping of electrons of TiO_2 from the valence band to the conduction band by photons.[140] The stimulus conditions convert the composites from the deswelling state to swelling and bacteria can easily reach TiO_2 nanoparticles. In other wands, more content of TiO_2 releases from the composite in swelling state. Therefore, the antibacterial activity of composites is greater in the swelling state than in the deswelling state. The presence of light facilitates jumping of the valence electrons from the valence band to the conduction band. Therefore, the antibacterial activity of composites is greater in the presence of sunlight than in the darkness. The synergistic effect of both TiO_2 and polymers also affects the antibacterial performance of TPC.

5.4. Removal of pollutants *via* adsorption

TiO_2 nanoparticles are studied as excellent adsorbents due to their sensitive surface reactivity,[148] controlled size particles,[149]

textural features,[150] and favorable zero-point-charge (pH_{pzc} = 6.8–7.6).[151] The pH_{zpc} is the pH value at which no charge is present in the structure of TPC. These properties of TiO_2 make them capable of interacting with pollutants. Therefore, TiO_2 can act as an adsorbent for the removal of pollutants, as shown in Fig. 8. Similarly, crosslinked polymers can also be used as adsorbents for the removal of pollutants. The crosslinked organic structures have polar and non-polar moieties in their structures which make them suitable for adsorption due to electrostatic interaction.[152] The composites of TiO_2 particles and crosslinked organic polymers have both (TiO_2 and organic polymers) characteristics which make the TPC as a perfect adsorbent. Therefore, the adsorptive property of TiO_2 particles is further enhanced by making composites with crosslinked organic polymers.[27] The adsorptive property of TiO_2–polymer composites is greater than individuals of both TiO_2 nanoparticles[127] and crosslinked organic polymers.[46] The adsorption of pollutants has occurred due to electrostatic, dipole–dipole, n–π interactions and hydrogen bonding which can be altered by varying the environment of medium,[121,125] nature of adsorbent,[3] and nature of adsorbents.[34] The adsorptive property of TiO_2–polymer composites can be enhanced with the help of the following factors, as shown in Fig. 9.

The adsorption capacity of TiO_2–polymer composites is greatly influenced by the temperature of the surrounding environment.[71,102] As discussed before, hydrophilic interactions are greater than hydrophobic interactions at low temperatures. The temperature above which the hydrodynamic radius of crosslinked polymers rapidly decreases is called volume phase transition temperature (VPTT). Therefore, the structures of composites are present in swelling state (at $T \leq$ VPTT). Therefore, more content of pollutants can adsorb on the surface of composites at $T \leq$ VPTT as reported by Zhou *et al.*[102] Furthermore, hydrophilic interactions are weaker than hydrophobic interactions at high temperatures (at $T \geq$ VPTT). Therefore, the structures of composites are present in a deswelling state. Therefore, the area of available space is very low. Therefore, very small amounts of pollutant can adsorb on the surface of adsorbents. In conclusion, more pollutants are adsorbed by TiO_2–polymer composites at $T \leq$ VPTT and less at $T \geq$ VPTT as shown in Fig. 9(b). Such behavior is observed only in those composites which have temperature-sensitive moieties in their structures. In the case of absence of temperature sensitive composites in structures, then the adsorption capacity increases with the increase in temperature due to increase in the number of collisions, as reported by Binaeian *et al.*[21]

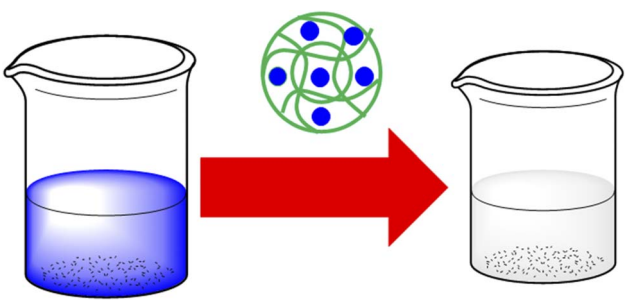

Fig. 8 Adsorption of pollutants by TPC.

The porosity of TiO_2–polymer composites is also an important factor in adsorption capacity of adsorbents. If large porosity is present in the structure of adsorbents, then more empty space is available for capturing the adsorbate. While low space is available for capturing if porosity of adsorbents is low. Therefore, the adsorption capacity of TiO_2–polymer composites can be enhanced by introducing more porosity. The porosity of organic polymers increases with the insertion of TiO_2 into the structure of crosslinked organic polymers.[139] Therefore, the adsorption capacity of composites is greater than crosslinked organic polymers, as reported by Barak *et al.*[61] The porosity of composites depends on the content of TiO_2 in composites. More porosity is present at high content of TiO_2 and low at low content of TiO_2. In simple words, the adsorption capacity of composites can be enhanced by increasing the content of TiO_2 nanoparticles in composites as reported by Naserzade *et al.*[27]

The mobility of water molecules into and out of the structure of TiO_2–polymer composites also plays a critical role in their adsorption capacity. This movement involves the entrance and outlet of pollutants across the crosslinked network of TiO_2–polymer composites along with water molecules. Initially, pollutants adhere to the surface of the composites before penetrating the crosslinked network, leaving behind empty spaces that subsequent pollutant molecules occupy. Consequently, the adsorption capability of composites depends on this penetration of pollutants from the surface. Hence, the mobility in the structure of composites directly impacts their adsorption efficiency. This mobility is maximum at the swelling state of composite and diminishes by shifting from a swelling state to a deswelling state.[39]

In the swollen state, mobility occurs easily due to sufficient empty space within the structure of composites. Conversely, as the shifting from swelling state to a shrunken one, these available spaces decrease, resulting in restriction of pollutant mobility as reported by Samanta *et al.*[70] Consequently, the adsorption capacity of composites declines. The adsorption capacity of TiO_2–polymer composites is significantly influenced by the pH value of the solution. This factor plays a critical role in adsorption capacity of TiO_2–polymer composites due to varying the structure of both the adsorbent and the adsorbate. The pH value at which no charge is present in the structure of composites is called pH at zero-point-charge (pH_{zpc}). TiO_2–polymer composites which have acidic (–COOH, $–SO_3H$) groups in their structure are called acidic TiO_2–polymer composites while those composites which have basic ($–NH_2$, –NH–) groups are called basic TiO_2–polymer composites. When the pH of the medium changes from pH_{zpc} value, the structure of composites can accept or donate protons. Acidic composites donate protons from their structure at pH ≥ pH_{zpc}, leading to the formation of anions while at pH ≤ pH_{zpc}, the acidic composites accept their released protons from acidic medium and shift in the neutral forms. The anionic form (acidic composites in a basic medium (pH ≥ pH_{zpc})) of acidic composites exhibits a strong affinity for cationic pollutants due to strong electrostatic interactions developing from opposite charges while repel the anionic

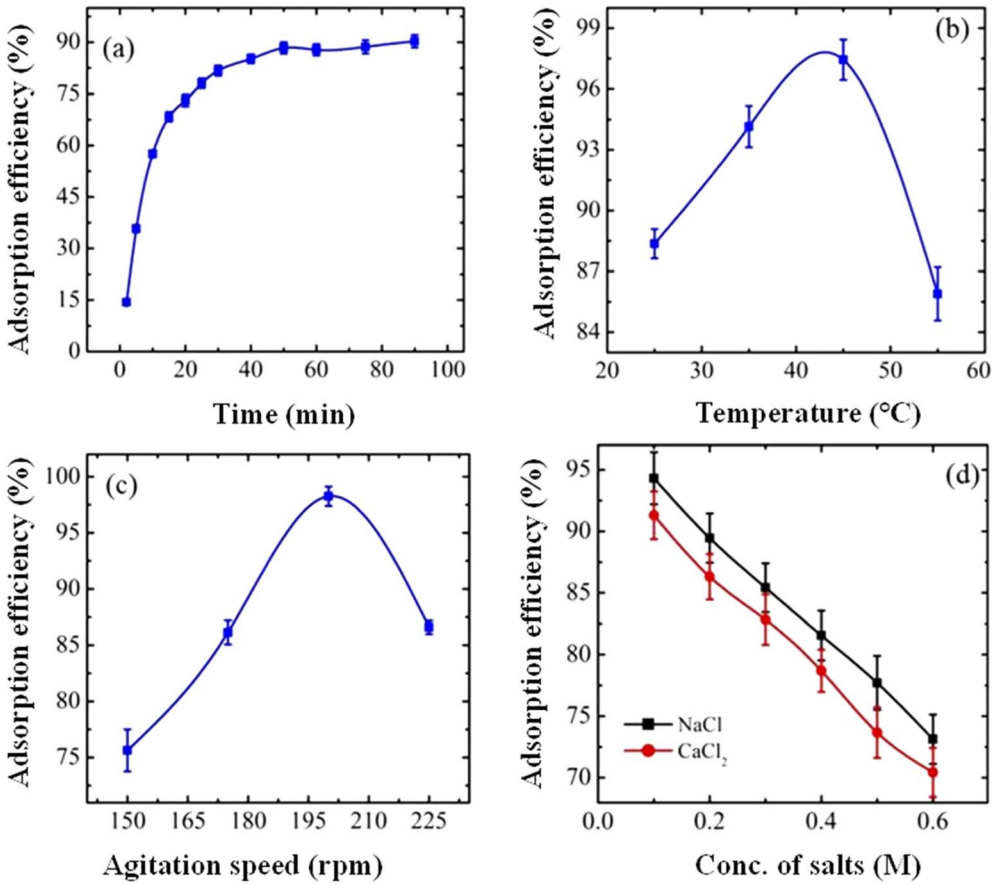

Fig. 9 Effect of parameters on the adsorption of pollutants: (a) contact time, (b) temperature, (c) agitation speed, and (d) salt concentrations (reproduced from ref. 132 with permission from Elsevier, copyright 2016).[132]

pollutants due to similar charges.[126,145,153] Similarly, basic composites acquire positive charges within their structure by accepting protons at pH $\leq$ pH_{zpc} and present donate the accepted proton from their structure at pH $\geq$ pH_{zpc}.[144] Therefore, basic composites in their cationic form interact with anionic pollutants because of the opposing charges present on both the adsorbent (basic composites) and adsorbate (pollutants) species. Consequently, the pH of the medium profoundly influences the interactions between adsorbate and absorbent species.

Similarly, the value of pH of the medium influences both the configuration and electronic distribution of pollutants. When the medium is basic, acidic dyes release their protons, while basic dyes receive protons under acidic conditions. Consequently, this alteration in the charge within the structure of pollutants leads to changes in electrostatic interactions between the composites and pollutants, as reported by Patel *et al.*[153] Moreover, metal cations produce the insoluble metal hydroxides in a basic medium, thereby reducing the presence of metal cations in the medium.[126] As a result, the adsorption efficiency of composites decreases for metal cations due to this phenomenon.

The adsorbed amount of pollutant can be increased with the increase in the contact time, as shown in Fig. 9(a). Initially, the adsorption process of pollutants on the composites increases rapidly due to a higher availability of functional groups on their surface for interaction with pollutants. However, after a certain period, the removal of pollutants by the composites begins to occur at a slower rate. This is due to the occupation of all active sites or functional groups of composites by pollutants, leaving no vacant sites for further adsorption. At this stage, the inner functional groups of composites interact with the adsorbed pollutants from the surface, facilitating the movement of pollutants towards the interior of the structure of composites through crosslinked networks. Consequently, the outer functional groups remain unoccupied, effectively halting further adsorption. This process follows the intraparticle diffusion mechanism, wherein pollutants diffuse within the structure of composites over time. Continuing onward, the extraction of pollutants gradually diminishes as the functional groups on the composites become saturated, reducing their capacity to adsorb additional pollutants. A stage comes at which the rate of adsorption on composites becomes equal to the rate of desorption of pollutants, as reported by Samanta *et al.*[70] This stage is called equilibrium position.[46]

Agitation speed and concentrations of different salts are also influenced on the adsorption capacity of TPC, as shown in Fig. 9(c) and (d) respectively. When the speed of agitation increases resulting in more adsorption capacity initially due to the rapid approach of pollutants to the TPC surface. This

adsorption efficiency decreases after a certain level of speed due to increase in the number of collisions which hinders the adsorption process. However, the effect of ionic salts is always decreasing the adsorption capacity of TPC. This is due to the interaction of metal cations with the structure of TPC. This interaction decreases the mobility of TPC by deswelling trends. This decreasing trend depends on the oxidation state of metal cations.[132]

5.5. Photocatalysis

Photocatalysis is an environmentally friendly and sustainable method which is used to disintegrate pollutants from water. This approach efficiently removes the pollutants from contaminated water without producing harmful byproducts.[41] In this process, the composites entirely break down the pollutants or transform them into harmless materials. The efficiency of photocatalytic remediation depends on the photocatalyst employed in an advanced oxidative process. These catalysts absorb photons possessing energy equivalent to or greater than the band gap energy between the valence and conduction bands of the photocatalyst.

The absorption of photons triggers a separation of charges caused by jumping of electrons from the valence band to the conduction band. During this movement of electrons, positive holes are created in the valence band.[143] These positive holes oxidize the water molecules to produce hydroxyl radicals ($OH^{\bullet}$) or directly target contaminants. While the excited electrons in the conduction band reduce the adsorbed oxygen molecules from the surface of photocatalyst (TiO_2–polymer composites). The resulting $OH^{\bullet}$ (at valence band) free radicals interact the contaminants to initiate diverse reactions that convert pollutants into non-toxic or harmless forms or completely degrade them into H_2O and CO_2 by oxidation[13] as shown in Fig. 10.

In TiO_2–polymer composites, TiO_2 nanoparticles are the main catalysts which proceed this phenomenon of adsorption of light and then used for excitation of electrons from the valence to the conduction band. The resulting electron–hole pairs degrade or transform the pollutants into non- or less toxic molecules. The pairs of electrons and holes have strong tendency to recombine and thus impact the overall efficiency of photocatalysis.[124] As a result, it becomes crucial to either control or reduce the recombination of these generated charge carriers to guarantee efficient photocatalytic reactions. The efficiency of TiO_2–polymer composites for degradation/transformation of pollutants from wastewater depends on several factors as shown in Fig. 11. These factors are given below.

The rate of catalytic degradation of pollutants by TiO_2–polymer composites can be tuned with varying the pH of the medium. The pH_{pzc} value of TiO_2 lies in the range of 6.8–7.6. This value can be changed by the influence of crosslinked structure of polymers due to interactions.[39,132] The pH of the medium greatly affects the protonated and deprotonated structures of TPC. This behavior depends on the nature of crosslinked polymers whether it is acidic or basic as shown in Fig. 11(b) and (e) respectively. The acidic structures have –COOH,[53] or $-SO_3H$[142] groups in their structure and basic have $-NH_2$ (ref. 103) in their structures. The polymeric network of acidic composites donates their protons to the medium at pH $\geq$ pK_a value of acidic composites and regains the released protons at pH $\leq$ pK_a. At pH $\geq$ pK_a, the acidic groups (–COOH, or $-SO_3H$) are converted into deprotonated ($-COO^-$, or $-SO_3^-$) forms. Under this condition, electrostatic repulsion occurs between the anionic structures of acidic composites due to same charges. Therefore, the hydrodynamic diameter of acidic composites increases. Therefore, the diffusion rate of pollutants increases across the crosslinked network to the surface of TiO_2. Thus, the degradation rate increases at pH $\geq$ pK_a value in acidic composites. While protonation occurred at pH $\leq$ pK_a and hence, the electrostatic repulsion diminishes. Therefore, the hydrodynamic diameter of composites decreases. Therefore, the rate of diffusion also decreases pollutants, resulting in a decline in the degradation rate of pollutants by acidic composites. Furthermore, the basic composites gain the protons from medium at pH $\leq$ pK_a and basic ($-NH_2$) groups of basic composites are converted into cationic ($-NH_3^+$) forms. In this condition, electrostatic repulsion also occurs due to same changes and the hydrodynamic diameter of basic composites

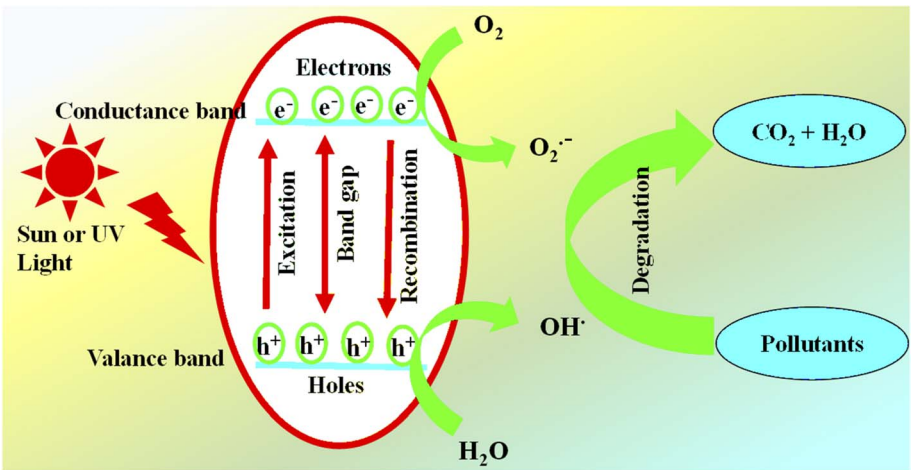

Fig. 10 Photocatalytic degradation mechanism.

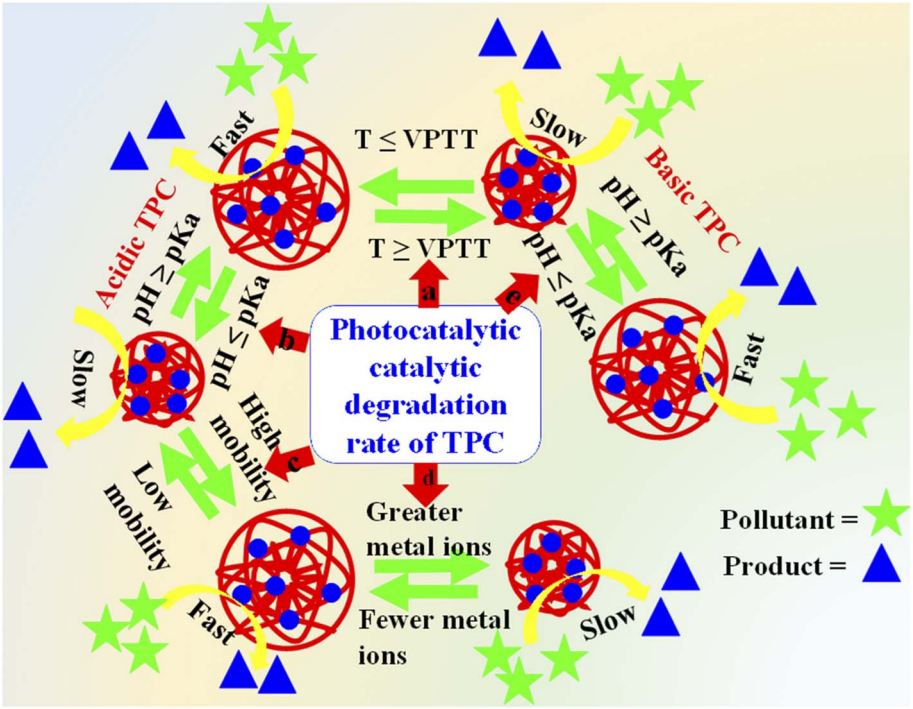

Fig. 11 Factors affecting the catalytic degradation efficiency of TPCs: (a) temperature, (b) pH in acidic TPCs, (c) mobility, (d) concentrations of metal cations and (e) pH in basic TPCs.

increases at pH ≤ pK_a. Therefore, catalytic degradation also increases because of the high diffusion rate of pollutants. While deprotonations occur at pH ≥ pK_a value and therefore, the hydrodynamic diameter decreases which causes the decline in catalytic efficiency of basic composites. The pH of medium also affects the structure of TiO_2. TiO_2 is present in neutral form as Ti–O–H at pH = 6.8. This value of TiO_2 is called zero potential charge which is represented as pH_{zpc}. TiO_2 is present in Ti–OH_2^+ at pH ≤ 6.8 and in Ti–O^- at pH ≥ 6.8 as reported by Gao *et al.*[75]

Content of TiO_2 particles also affects the catalytic efficiency of TiO_2–polymer composites. At high contents of TiO_2 in composites, more active sites are available for catalysis. Therefore, more pollutants can be adsorbed under this condition. Thus, the degradation rate of pollutants by TiO_2–polymer composites rises with the increase in the content if TiO_2 in composite forms as reported by Wei *et al.*[31] A similar trend for photocatalytic degradation of dye has been reported by Marija *et al.*[53]

Temperature also affects the catalytic performance of TiO_2–polymer composites as shown in Fig. 11(a). The photocatalytic degradation of pollutants occurs when valence electrons jump from valence band to conduction band. Therefore, this jumping rate of electrons depends on the value of temperature (intensity of light). If the intensity of light is high (high temperature), then more electrons jump from valence band to conduction band. Therefore, more electrons and holes pairs are produced in this result. These electron–hole pairs more rapidly degraded the pollutants from water. Furthermore, a smaller number of electron–hole pairs are formed at low intensity of light. Therefore, photocatalytic performance also decreases at low intensity of light. The increasing trend of photocatalytic efficiency is under increasing the power of light is up to a specific level in certain solvents. Beyond this level, the solvents can produce bubbles which produce hindrance for waves in the process of sonocatalytic degradation reactions only. Therefore, the degradation performance of TPC can be decreased. Similar trends are observed by Afzal *et al.*[13] The photocatalytic performance of TPC can be enhanced by using suitable light energy source. Generally, the photocatalytic activity of TPC is greater in sun light than other sources of energy as reported by Zhu *et al.*[113]

The recombination of electron–hole pairs decreases the catalytic efficiency of the TiO_2–polymer composites. This recombination of electron–hole pairs is controlled by doping of TiO_2 particles. This doping can be N-type or P-type. In P-type doping, cationic metal or three valence electrons containing atoms are added into the composites which further decreases the energy band gap of TiO_2. Therefore, the valence electrons easily jump from valence to conduction bands. Thus, degradation rate of pollutants increased by P-type doping of TPC. Similarly, the photocatalytic performance of composites is also enhanced by N-type doping. In this doping, the atoms which have five electrons in their valence shell or electron rich species are added into the composites. This doping also decreases the energy band gap of TiO_2 particles and hence, the photocatalytic activity increases due to easily jumping of electrons from valence to conduction bands. Liu *et al.*[105] have also observed similar increasing trends in photocatalytic performance of TPC by adding Fe^{3+} ions (P-type doping). Galata *et al.*[119] have also studied the photocatalytic performance of TPC by doping with

N-type and P-type materials. They observed increasing trends by both types of doping but more increasing in N-type doping.

The photocatalytic performance of composites can also be tuned with porosity of composites (greater porosity means greater mobility) as shown in Fig. 11(c). The photocatalytic activity of polymer composites is high when the porosity of composites is greater. This porosity controls the adsorptions of pollutants and then these adsorbed pollutants penetrated from the surface of crosslinked polymer to the surface of TiO_2 particles. Therefore, the porosity of composites controls the approach pollutants to the surface of TiO_2 particles. In this way, the porosity of composites controls the photocatalytic activity of composites. The porosity of composites can be enhanced by increasing the content of TiO_2,[120] or by increasing the content of monomers[154] or comonomers[42,43] during the synthesis of composites.

The content of acidic,[46] basic,[141] and polar[58] components in TiO_2–polymer composites also influence the photocatalytic efficiency. These components affect due to interaction (attraction (in case of opposite charges) or repulsion (in case of same charges)) with pollutants. If the content of these components is at a greater level, then more contents of oppositely charged pollutants are adsorbed and therefore, more molecules of pollutants reach to the surface of TiO_2 particles. Therefore, the efficiency of composites increased with the increase in the percentage of these components in composites.

The nature of pollutants[75] and TiO_2–polymer composites[39] also influence the photocatalytic efficiency of composites. Basically, their nature affects the interaction present between the pollutants and TPC. If the same charges are present in the structures of both composites and pollutants, then electrostatic repulsion occurs and photocatalytic performance decreases. Furthermore, if opposite charges are present in both pollutants and composites, then electrostatic interactions force the pollutants to come on the surface of TiO_2. Therefore, the efficiency of composites can be tuned with respect to the nature of organic polymer and pollutants. Song *et al.*[112] have reported the effect of adsorbent and Sawut *et al.*[58] have the effect of nature of TPC on photocatalytic performance.

The photocatalytic efficiency of composites can also be controlled in various solvents. These solvents also interact the composites as well as pollutants. Therefore, these interactions also influence the interactions of composites with pollutants. If the interactions of solvents are greater than the interactions present between composites and pollutants, then the approaches of pollutants to the surface of TiO_2 particles reduce. Therefore, the photocatalytic efficiency of composites decreases. Pasaribu *et al.*[94] have also observed the effect of solvents on photocatalytic performance of TPC under isopropanol, ethanol, and DMSO solvents. The swelling of TPC was obtained in aprotic solvents and less in protic solvents due to hydrogen bonding. This swelling behavior controls the mobility of pollutants and consequently the photocatalytic performance of TPC.

The photocatalytic efficiency of TPC can be influenced by introducing the metal salts during the photocatalysis, as shown in Fig. 11(d). The metal ions, which are added into the mixture during photocatalysis, basically affect the interaction present between TPC and pollutants. Generally, the metal cations decrease the interactions between TPC and pollutants due to string interactions of metal cations with TPC. Therefore, the possibility of pollutants reaching the surface of TiO_2 particles decreases. Therefore, the catalytic efficiency of TPC decreases with the introduction of metal cations. The interaction of TPC is stronger with more metal cations having more oxidation states. Therefore, the photocatalytic activity is more significant with the introduction of higher oxidation state containing metal cations than lower oxidations containing. A similar trend has been reported by Patel *et al.*[153] Similarly, the anionic parts of salts also affect the interactions between TPC and pollutants. These anionic components also trap the OH radicals which results to decreases the degradation rate of pollutants as reported by Afzal *et al.*[13]

5.6. Other applications

TiO_2–polymer composites can also be employed in some other fields of research. For example, TiO_2–polymer composites are used for the fabrication of clothes,[24] engineering of tissues,[60] selectively rejection of protein,[155] detection of Fe^{3+} ions[84] and high puncture resistant along with self-healing.[156] The fabrication of clothes with TPC is a very important application. This application protects human health from diseases due to antibacterial and ultraviolet protection properties. These properties are basically due to the presence of TiO_2 particles. TiO_2 particles can absorb ultraviolet radiation and protect the human body from their hazardous effects. The engineering of tissue application of TPC is also very important. During the injury, the interactions which are essential for connection are disturbed. The TPC facilitates rejoining the parts or cells for healing as well as killing the bacteria. In this way, the TPC helps to heal the injuries as reported by Niranjan *et al.*[33] and Motasadizadeh *et al.*[40] This healing property is also very fruitful for punctures. The strong interaction resists breaking their components. Therefore, TPC shows high resistance against punctures. The selectivity of TPC for suitable species is also very important, which is generated with the help of the crosslinked network. The structure of polymer play an important role in this selectivity due to electrostatic repulsions on the basis of same charges and interactions on the basis of opposite charges as reported by Gao *et al.*[155] The detection property of TPC also depends on the crosslinked network. This crosslinked network makes co-ordinate covalent bonds with metal ions. Due to this bond formation, the color of metal ions changes, which indicates the presence of corresponding metal ions.

6. Summary and future directions

Metal oxides and polymers are widely used in various applications. Their combined behavior opens new avenues in different fields. The composites of TiO_2 and crosslinked organic polymers are very important with respect to their applications. In this review, TiO_2–polymer composites are classified based on morphology and nature of crosslinker. The synthetic

approaches used for the synthesis of TiO_2–polymer composites are also discussed in detail. The morphology of these composites is very important with respect to their applications which are identified with various techniques as explained in this review article. TiO_2–polymer composites have various applications but the most important are the antibacterial and removal of pollutants from water through both photocatalysis and adsorption processes. The TPC with covalent crosslinker has more advantage over TPC formed by H-bonding. The hydrogen bonding of TPC can also vanish under certain conditions. However, the TPC in which the crosslinker is covalently bonded is stable for a long time.

TiO_2–polymer composites are more suitable materials for antibacterial activities, but the polymer systems which are used consist of mostly *N*-isopropylacrylamide which is a non-biodegradable material. Therefore, it is harmful to the health. This should be replaced with a biodegradable material which is non-toxic for health. This development opens new doors for their applications in medicine. The adsorption of pollutants greatly depends on the polymer materials. For this purpose, the polar monomers and comonomers are efficient for this purpose. The insertion of acidic (–COOH, $-SO_3H$) and basic ($-NH_2$) groups play a vital role in enhancing the adsorption and rejection of pollutants from water. Their performance increases even more with changing the pH of the medium. The adsorption performance is also effects by medium which is not reported yet. The mean challenge in the photocatalytic activity of TiO_2–polymer composites is the electron–hole pair recombination. This issue of catalytic performance can be resolved by doping the TiO_2 particles. Therefore, the doping materials decrease the energy band gap along with preventing the recombination of electrons and holes of TiO_2 particles.

The reported morphology of TiO_2–polymer composites is mostly homogenous microsphere. More work should be done on other morphologies such as core–shell and hollow systems. These morphologies are more effective with respect to homogenous microphase. However, synthesis and applications of such morphological composites are not reported in the literature. These classes open new avenues for research in TiO_2–polymer composites. These core shell systems in which core is made with solid materials have more effective than homogenous composite microspheres due to easily recyclable property (due to more density). Similarly, the core–shell systems in which TiO_2 nanoparticles are present as core are more effective due to controlling the leakage of TiO_2 nanoparticles during recycling than homogenous composites microspheres. Furthermore, hollow composites are also more effective than homogenous composites with respect to adsorption and photocatalytic degradation/transformation reactions of pollutants. In hollow spheres, the pollutants can enter the crosslinked network of composites from both sides (interior and exterior sides). Therefore, the pollutants can easily be approached to the TiO_2 nanoparticles present in the hollow composite spheres. As a result, the photocatalytic activity and adsorption of pollutants of hollow composites should be greater than other morphologies. Hollow composites can also be more suitable in drug delivery due to maximum releasing of loaded drug. Other systems partially released the loaded drug, but hollow systems should be released greater loaded amount through both sides (interior and exterior sides).

Abbreviations

AAc	Acrylic acid
NIPAM	*N*-Isopropylacrylamide
SoA	Sodium alginate
NPs	Nanoparticles
P(Q-10)	Polyquaternium-10
AAm	Acrylamide
DMAAm	*N*,*N*′-Dimethylacrylamide
GG	Gum ghatti
P(VA)	Poly(vinyl alcohol)
DLS	Dynamic light scattering
CS	Chitosan
P(EOAAm)	Ethylene oxide-polyacrylamide
EDX	Energy dispersive X-rays
KCG	K-Carrageenan
FTIR	Fourier Transformed Infrared Spectroscopy
XG	Xanthan gum
HRTEM	High resolution transmission electron microscopy
GeG	Gellan gum
VP	Vinyl pyrrolidone
PoA	Potassium acrylate
HPMC	Hydroxypropyl methylcellulose
NMBA	*N*,*N*′-Methylene-bisacrylamide
AmPS	Ammonium persulfate
AMPS	2-Acrylamido-2-methylpropane sulphonic acid
HEMA	2-Hydroxyethyl methacrylate
IA	Itaconic acid
TPC	TiO_2–polymer composites
SEM	Scanning electron microscopy
MAAn	Methacrylic anhydride
EGDA	Ethylene-glycol-diacrylate
MAAc	Methacrylic acid
TGA	Thermo gravimetric analysis
NTMEDA	*N*,*N*,*N*′,*N*′-Tetramethylenethylendiamince
GX	Glyoxal
UV-vis	UV/visible spectroscopy
VPTT	Volume phase transition temperature
GO-P(NDMAAm)	Graphene oxide-poly(*N*,*N*′-dimethylacrylamide)
XPS	X-ray photoelectron spectroscopy
PoPS	Potassium persulfate
XRD	X-ray diffraction
ICP-AES	Inductively coupled plasma-atomic emission spectroscopy

Data availability

Data will be provided on request.

Conflicts of interest

There is no conflict of interest.

Acknowledgements

Muhammad Arif is thankful to University of Management and Technology, Lahore-54770, Pakistan.

References

1 R. Reddy Nagavally, *Composite Materials-History, Types, Fabrication Techniques, Advantages, and Applications*, 2016.
2 M. F. Ashby, *Acta Metall. Mater.*, 1993, **41**, 1313–1335.
3 S. Marouch, N. Benbellat, A. Duran and E. Yilmaz, *ACS Omega*, 2022, **7**, 35256–35268.
4 M. Arif, *Mater. Today Commun.*, 2023, **36**, 106580.
5 H. Zhang, P. Tang, K. Yang, Q. Wang, W. Feng and Y. Tang, *Desalination*, 2023, **558**, 116620.
6 M. Arif, A. Rauf, H. Raza, S. Ben Moussa, S. M. Haroon, A. Y. A. Alzahrani and T. Akhter, *Int. J. Biol. Macromol.*, 2024, **275**, 133633.
7 M. Arif, A. Rauf and T. Akhter, *Int. J. Biol. Macromol.*, 2024, **274**, 133250.
8 M. Arif, H. Raza, S. M. Haroon, S. Ben Moussa, F. Tahir and A. Y. A. Alzahrani, *Int. J. Biol. Macromol.*, 2024, **270**, 132331.
9 M. Arif, *J. Environ. Chem. Eng.*, 2023, **11**, 109270.
10 M. Arif, M. Shahid, A. Irfan, J. Nisar, X. Wang, N. Batool, M. Ali, Z. H. Farooqi and R. Begum, *Z. Phys. Chem.*, 2022, **236**, 1219–1241.
11 M. Arif, M. Shahid, A. Irfan, J. Nisar, W. Wu, Z. H. Farooqi and R. Begum, *RSC Adv.*, 2022, **12**, 5105–5117.
12 M. Arif, *J. Mol. Liq.*, 2023, **375**, 121346.
13 M. Z. Afzal, P. Zu, C. M. Zhang, J. Guan, C. Song, X. F. Sun and S. G. Wang, *J. Hazard. Mater.*, 2022, **434**, 128879.
14 M. Arif, *RSC Adv.*, 2023, **13**, 3008–3019.
15 M. Arif, *J. Mol. Liq.*, 2024, **403**, 124869.
16 M. Arif, *JOM*, 2024, **76**, 1203–1222.
17 M. Arif, *Eur. Polym. J.*, 2024, **206**, 112803.
18 M. Arif, H. Raza and T. Akhter, *RSC Adv.*, 2024, **14**, 24604–24630.
19 M. Arif, A. Rauf and T. Akhter, *RSC Adv.*, 2024, **14**, 19381–19399.
20 M. Arif, *RSC Adv.*, 2024, **14**, 9445–9471.
21 E. Binaeian, S. Babaee Zadvarzi and D. Yuan, *Int. J. Biol. Macromol.*, 2020, **162**, 150–162.
22 M. Arif, *RSC Adv.*, 2022, **12**(24), 15447–15460.
23 H. Zhang, R. Shi, A. Xie, J. Li, L. Chen, P. Chen, S. Li, F. Huang and Y. Shen, *ACS Appl. Mater. Interfaces*, 2013, **5**, 12317–12322.
24 A. L. Mohamed and A. G. Hassabo, *J. Polym. Res.*, 2022, **29**, 1–18.
25 A. S. Montaser, A. R. Wassel and O. N. Al-Shaye'a, *Int. J. Biol. Macromol.*, 2019, **124**, 802–809.
26 R. R. Mansurov, V. S. Zverev and A. P. Safronov, *J. Catal.*, 2022, **406**, 9–18.
27 S. M. Naserzade, M. Shahrousvand, J. Mohammadi-Rovshandeh and H. Basati, *J. Polym. Environ.*, 2023, **31**, 2014–2031.
28 M. Madani, N. Sharifi-Sanjani, A. Hasan-Kaviar, M. Choghazardi, R. Faridi-Majidi and A. S. Hamouda, *Polym. Eng. Sci.*, 2013, **53**, 2407–2412.
29 A. Taniguchi and M. Cakmak, *Polymer*, 2004, **45**, 6647–6654.
30 S. Thakur and O. Arotiba, *Adsorpt. Sci. Technol.*, 2018, **36**, 458–477.
31 S. Wei, X. Zhang, K. Zhao, Y. Fu, Z. Li, B. Lin and J. Wei, *Polym. Compos.*, 2016, **37**, 1292–1301.
32 H. Zhang, J. Zhu, Y. Hu, A. Chen, L. Zhou, H. Gao, Y. Liu and S. Liu, *J. Nanomater.*, 2019, **2019**(1), 2326042.
33 R. Niranjan, M. Kaushik, R. T. Selvi, J. Prakash, K. S. Venkataprasanna, D. Prema, B. Pannerselvam and G. D. Venkatasubbu, *Int. J. Biol. Macromol.*, 2019, **138**, 704–717.
34 M. Lučić, N. Milosavljević, M. Radetić, Z. Šaponjić, M. Radoičić and M. K. Krušić, *Sep. Purif. Technol.*, 2014, **122**, 206–216.
35 R. El Kaim Billah, A. Shekhawat, S. Mansouri, H. Majdoubi, M. Agunaou, A. Soufiane and R. Jugade, *Environ. Nanotechnol. Monit. Manag.*, 2022, **18**, 100695.
36 A. M. Aljeboree, N. D. Radia, L. S. Jasim, A. A. Alwarthan, M. M. Khadhim, A. Washeel Salman and A. F. Alkaim, *J. Ind. Eng. Chem.*, 2022, **109**, 475–485.
37 M. Çapkın Yurtsever and G. Güldağ, *J. Mech. Behav. Biomed. Mater.*, 2023, **146**, 106088.
38 C. A. Coutinho, R. K. Harrinauth and V. K. Gupta, *Colloids Surf. A Physicochem. Eng. Asp.*, 2008, **318**, 111–121.
39 T. D. Kusworo, M. Yulfarida, A. C. Kumoro and D. P. Utomo, *Chin. J. Chem. Eng.*, 2023, **55**, 123–136.
40 H. Motasadizadeh, S. Azizi, A. Shaabani, M. G. Sarvestani, R. Sedghi and R. Dinarvand, *Carbohydr. Polym.*, 2022, **296**, 119956.
41 L. Midya, A. N. Sarkar, R. Das, A. Maity and S. Pal, *Int. J. Biol. Macromol.*, 2020, **164**, 3676–3686.
42 Y. E. Moon, G. Jung, J. Yun and H. Il Kim, *Mater. Sci. Eng. B*, 2013, **178**, 1097–1103.
43 S. Jeon, J. Yun, Y. S. Lee and H. Il Kim, *J. Ind. Eng. Chem.*, 2012, **18**, 487–491.
44 H. Si, L. Zhou, Y. Wu, L. Song, M. Kang, X. Zhao and M. Chen, *Compos. B Eng.*, 2020, **199**, 108278.
45 A. H. Jawad and M. A. Nawi, *Carbohydr. Polym.*, 2012, **90**, 87–94.
46 A. M. Elbarbary and Y. H. Gad, *Int. J. Environ. Anal. Chem.*, 2023, DOI: **10.1080/03067319.2023.2198646**.
47 C. Xiao, Y. Fang and G. Zhang, *Polym. Compos.*, 2017, **38**, 132–137.
48 M. Arif, Z. H. Farooqi, A. Irfan and R. Begum, *J. Mol. Liq.*, 2021, **336**, 116270.
49 K. Naseem, R. Begum and Z. H. Farooqi, *Polym. Compos.*, 2018, **39**, 2167–2180.
50 M. Arif, *Polymers*, 2023, **15**, 3600.
51 M. Shahid, Z. H. Farooqi, R. Begum, M. Arif, M. Azam, A. Irfan and U. Farooq, *Z. Phys. Chem.*, 2022, **236**, 87–105.
52 S. Xu, Z. Qian, N. Zhao and W. Yuan, *J. Colloid Interface Sci.*, 2024, **654**, 1431–1446.
53 L. Marija, M. Nedeljko, R. Maja, Š. Zoran, R. Marija and K. K. Melina, *Polym. Compos.*, 2014, **35**, 806–815.

54 M. N. Birkholz, G. Agrawal, C. Bergmann, R. Schröder, S. J. Lechner, A. Pich and H. Fischer, *Biomed. Tech.*, 2016, **61**, 267–279.
55 C. Vakifahmetoglu, D. Zeydanli and P. Colombo, *Mater. Sci. Eng. R Rep.*, 2016, **106**, 1–30.
56 K. Kulbaba, A. Cheng, A. Bartole, S. Greenberg, R. Resendes, N. Coombs, A. Safa-Sefat, J. E. Greedan, H. D. H. Stöver, G. A. Ozin and I. Manners, *J. Am. Chem. Soc.*, 2002, **124**, 12522–12534.
57 M. Ranjbar-Mohammadi, M. Rahimdokht and E. Pajootan, *Int. J. Biol. Macromol.*, 2019, **134**, 967–975.
58 A. Sawut, T. Wu, R. Simayi, T. Wu, X. Gong and Z. Wang, *Colloids Surf., A*, 2023, **678**, 132531.
59 J. Wen, X. Li, H. Zhang, S. Zheng, C. Yi, L. Yang and J. Shi, *Sep. Purif. Technol.*, 2023, **304**, 122403.
60 K. Zazakowny, J. Lewandowska-Łańcucka, J. Mastalska-Popławska, K. Kamiński, A. Kusior, M. Radecka and M. Nowakowska, *Colloids Surf., B*, 2016, **148**, 607–614.
61 A. Barak, Y. Goel, R. Kumar and S. K. Shukla, *Mater. Today: Proc.*, 2019, **12**, 529–535.
62 S. K. Samanta, B. Mandal and T. Tripathy, *J. Appl. Polym. Sci.*, 2022, **139**, e52465.
63 M. R. Mohammadi, M. C. Cordero-Cabrera, D. J. Fray and M. Ghorbani, *Sens. Actuators, B*, 2006, **120**, 86–95.
64 D. M. González-García, L. Téllez Jurado, R. Jiménez-Gallegos and L. M. Rodríguez-Lorenzo, *Mater. Sci. Eng., C*, 2017, **75**, 375–384.
65 S. Banerjee, D. D. Dionysiou and S. C. Pillai, *Appl. Catal., B*, 2015, **176–177**, 396–428.
66 W. Zhou, F. Sun, K. Pan, G. Tian, B. Jiang, Z. Ren, C. Tian and H. Fu, *Adv. Funct. Mater.*, 2011, **21**, 1922–1930.
67 S. Khalilian, S. Abdolmohammadi and F. Nematolahi, *Lett. Org. Chem.*, 2017, **14**(5), 361–367.
68 S. min Chang and W. szu Liu, *Appl. Catal., B*, 2011, **101**, 333–342.
69 M. R. Khafaga, H. E. Ali and A. W. M. El-Naggar, *J. Text. Inst.*, 2016, **107**, 766–773.
70 S. K. Samanta, B. Mandal and T. Tripathy, *J. Appl. Polym. Sci.*, 2022, **139**, e52465.
71 E. Makhado, B. R. Motshabi, D. Allouss, K. E. Ramohlola, K. D. Modibane, M. J. Hato, R. M. Jugade, F. Shaik and S. Pandey, *Chemosphere*, 2022, **306**, 135524.
72 J. Radwan-Pragłowska, M. Piątkowski, Ł. Janus, D. Bogdał, D. Matysek and V. Čablik, *Int. J. Polym. Mater. Polym. Biomater.*, 2019, **68**, 881–890.
73 E. P. Da Silva, M. R. Guilherme, F. P. Garcia, C. V. Nakamura, L. Cardozo-Filho, C. G. Alonso, A. F. Rubira and M. H. Kunita, *RSC Adv.*, 2016, **6**, 19060–19068.
74 Z. Zhang, Y. M. Katba Bader, J. Yang and L. A. Lucia, *J. Mol. Liq.*, 2021, **328**, 115332.
75 Y. Gao, S. Gu, L. Duan, Y. Wang and G. Gao, *Soft Matter*, 2019, **15**, 3897–3905.
76 C. A. Coutinho, R. K. Harrinauth and V. K. Gupta, *Colloids Surf., A*, 2008, **318**, 111–121.
77 C. C. Oey, A. B. Djurišić, H. Wang, K. K. Y. Man, W. K. Chan, M. H. Xie, Y. H. Leung, A. Pandey, J. M. Nunzi and P. C. Chui, *Nanotechnology*, 2006, **17**, 706.
78 J. Qiu, S. Zhang and H. Zhao, *Sens. Actuators, B*, 2011, **160**, 875–890.
79 G. Gülşen and M. Naci Inci, *Opt. Mater.*, 2002, **18**, 373–381.
80 H. Choi, S. R. Al-Abed, D. D. Dionysiou, E. Stathatos and P. Lianos, *Sustainability Science and Engineering*, 2010, **2**, 229–254.
81 Y. Yue, X. Wang, Q. Wu, J. Han and J. Jiang, *J. Colloid Interface Sci.*, 2020, **564**, 99–112.
82 M. R. Khafaga, H. E. Ali and A. W. M. El-Naggar, *J. Text. Inst.*, 2016, **107**, 766–773.
83 G. Taşkın Çakıcı, *Polym. Bull.*, 2023, **80**, 12719–12740.
84 S. Turk, B. ÃœnlÃ¼ and M. S. Mustapa, *International Journal of Integrated Engineering*, 2021, **13**, 266–273.
85 C. Cazan, A. Enesca, L. Isac, L. Andronic and M. Cosnita, *ACS Appl. Polym. Mater.*, 2023, **5**, 3958–3970.
86 H. Zhang, H. Yang, B. Shentu, S. Chen and M. Chen, *J. Appl. Polym. Sci.*, 2018, **135**, 46099.
87 M. Liao, Z. Liu, Y. Gao, L. Liu and S. Xiang, *Constr. Build. Mater.*, 2021, **301**, 124108.
88 A. Ayati, A. Ahmadpour, F. F. Bamoharram, B. Tanhaei, M. Mänttäri and M. Sillanpää, *Chemosphere*, 2014, **107**, 163–174.
89 S. M. Gupta and M. Tripathi, *Cent. Eur. J. Chem.*, 2012, **10**, 279–294.
90 P. C. Chen, C. C. Chen and S. H. Chen, *Curr. Nanosci.*, 2017, **13**(4), 373–393.
91 M. Karg, A. Pich, T. Hellweg, T. Hoare, L. A. Lyon, J. J. Crassous, D. Suzuki, R. A. Gumerov, S. Schneider, I. I. Potemkin and W. Richtering, *Langmuir*, 2019, **35**, 6231–6255.
92 G. Agrawal and R. Agrawal, *Small*, 2018, **14**, 1801724.
93 R. Begum, Z. H. Farooqi, E. Ahmed, A. Sharif, W. Wu and A. Irfan, *RSC Adv.*, 2019, **9**, 13838–13854.
94 S. P. Pasaribu, I. Masmur and A. S. Panggabean, *Mater. Chem. Phys.*, 2023, **305**, 127875.
95 D. Wang, Y. Tan, H. Xu, X. Wang, L. Yu, Z. Xiao, J. Wang and S. Xu, *Appl. Surf. Sci.*, 2019, **467–468**, 588–595.
96 S. Si, R. Zhou, Z. Xing, H. Xu, Y. Cai and Q. Zhang, *Fibers Polym.*, 2013, **14**, 982–989.
97 S. Senol and E. Akyol, *Mater. Sci.-Pol.*, 2021, **38**, 443–449.
98 H. Ritonga, M. I. Basri, F. S. Rembon, L. O. A. Nur Ramadhan and M. Nurdin, *Soil Sci. Annu.*, 2020, **71**, 194–204.
99 *Synthesis and Characterization of Nano-TiO2/Poly(N-isopropylacrylamide) Com-posite Hydrogels*, **http://sioc-journal.cn/Jwk_hxxb/EN/Y2007/V65/I21/2437**, accessed 9 January 2024.
100 M. Mostakhdemin, A. Nand, M. Arjmandi and M. Ramezani, *Mater. Today Commun.*, 2020, **25**, 101279.
101 C. Boztepe, M. Daskin, A. Erdogan and T. Sarici, *Polym. Eng. Sci.*, 2021, **61**, 2083–2096.
102 J. Zhou, B. Hao, L. Wang, J. Ma and W. Cheng, *Sep. Purif. Technol.*, 2017, **176**, 193–199.

103 J. Yun, D. Jin, Y. S. Lee and H. Il Kim, *Mater. Lett.*, 2010, **64**, 2431–2434.
104 M. M. Babić Radić, V. V. Filipović, J. S. Vuković, M. Vukomanović, T. Ilic-Tomic, J. Nikodinovic-Runic and S. L. Tomić, *Polymers*, 2023, **15**(7), 1643.
105 Y. G. Liu, X. J. Hu, H. Wang, A. W. Chen, S. M. Liu, Y. M. Guo, Y. He, X. Hu, J. Li, S. H. Liu, Y. Q. Wang and L. Zhou, *Chem. Eng. J.*, 2013, **226**, 131–138.
106 L. Zhang, S. Zhang, B. He, Z. Wu and Z. Zhang, *Z. Naturforsch. B Chem. Sci.*, 2008, **63**, 973–976.
107 X. You, H. Huang, R. Zhang, Z. Yang, M. Xu, X. Wang and Y. Yao, *Catalysts*, 2021, **11**, 613.
108 W. Kangwansupamonkon, W. Jitbunpot and S. Kiatkamjornwong, *Polym. Degrad. Stab.*, 2010, **95**, 1894–1902.
109 D. Gao, X. Wei, Y. Zhang, Y. Ma, G. Wang, X. Zhao, K. Liu, Y. Huo, H. Wang and B. Wang, *J. Dispersion Sci. Technol.*, 2021, **42**, 537–545.
110 H. M. Nizam El-Din, M. R. Khafaga and A. W. M. El-Naggar, *J. Macromol. Sci., Part A: Pure Appl. Chem.*, 2015, **52**, 821–829.
111 B. Xu, H. Li, Y. Wang, G. Zhang and Q. Zhang, *RSC Adv.*, 2013, **3**, 7233–7236.
112 X. F. Song, J. T. Qin, T. T. Li, G. Liu, X. X. Xia, Y. S. Li and Y. Liu, *J. Appl. Polym. Sci.*, 2020, **137**(13), 48516.
113 H. Zhu, R. Jiang, L. Xiao, L. Liu, C. Cao and G. Zeng, *Appl. Surf. Sci.*, 2013, **273**, 661–669.
114 F. O. Gokmen, S. Temel and E. Yaman, *Eur. Sci. J.*, 2019, **15**(33), 1857–7881.
115 R. Kandel, S. R. Jang, S. Shrestha, S. Y. Lee, B. K. Shrestha, C. H. Park and C. sang Kim, *ACS Appl. Mater. Interfaces*, 2021, **13**, 47100–47117.
116 L. Cui, H. Li, J. Huang and D. Xiong, *Ceram. Int.*, 2021, **47**, 34970–34978.
117 M. Li, L. Gao, J. Chen, Y. Zhang, J. Wang, X. Lu, K. Duan, J. Weng and B. Feng, *Biomed. Mater.*, 2018, **13**(4), 045008.
118 L. Ye, C. Miao, M. A. Brook and R. Pelton, *Langmuir*, 2008, **24**, 9341–9343.
119 E. Galata, E. A. Georgakopoulou, M. E. Kassalia, N. Papadopoulou-Fermeli and E. A. Pavlatou, *Materials*, 2019, **12**(16), 2589.
120 H. A. Abd El-Rehim, E. S. A. Hegazy and D. A. Diaa, *React. Funct. Polym.*, 2012, **72**, 823–831.
121 M. Lučić Škorić, I. Terzić, N. Milosavljević, M. Radetić, Z. Šaponjić, M. Radoičić and M. Kalagasidis Krušić, *Eur. Polym. J.*, 2016, **82**, 57–70.
122 S. Mallakpour and M. Hatami, *Appl. Clay Sci.*, 2018, **163**, 235–248.
123 R. El Kaim Billah, A. Shekhawat, S. Mansouri, H. Majdoubi, M. Agunaou, A. Soufiane and R. Jugade, *Environ. Nanotechnol. Monit. Manag.*, 2022, **18**, 100695.
124 F. Kazemi, Z. Mohamadnia, B. Kaboudin and Z. Karimi, *J. Appl. Polym. Sci.*, 2016, **133**(19), 43386.
125 A. K. T. Mohammad, A. S. Abdulhameed and A. H. Jawad, *Int. J. Biol. Macromol.*, 2019, **129**, 98–109.
126 A. A. Hendy, E. E. Khozemy, G. A. Mahmoud, E. A. Saad and S. H. Sorror, *Egypt. J. Chem.*, 2019, **62**, 1785–1798.
127 Y. Y. Wei, X. T. Sun and Z. R. Xu, *Appl. Surf. Sci.*, 2018, **445**, 437–444.
128 D. Wu, M. Yi, H. Duan, J. Xu and Q. Wang, *Carbon*, 2016, **108**, 394–403.
129 X. Wang, X. Li, X. Yang, K. Lei and L. Wang, *Colloids Surf., B*, 2021, **197**, 111410.
130 B. Xu, H. Li, Y. Wang, G. Zhang and Q. Zhang, *Polym. Compos.*, 2016, **37**, 810–817.
131 X. Wang, D. Hu and J. Yang, *Chem. Mater.*, 2007, **19**, 2610–2621.
132 H. Mittal and S. S. Ray, *Int. J. Biol. Macromol.*, 2016, **88**, 66–80.
133 F. Khalid, A. S. Roy, A. Parveen and R. Castro-Muñoz, *J. Mater. Sci. Eng. B*, 2024, **299**, 116929.
134 F. I. A. El Fadl, D. E. Hegazy, N. A. Maziad and M. M. Ghobashy, *Int. J. Biol. Macromol.*, 2023, **250**, 126248.
135 R. Balasubramanian, S. S. Kim, J. Lee and J. Lee, *Int. J. Biol. Macromol.*, 2019, **123**, 1020–1027.
136 R. Surkatti, M. M. C. M. van Loosdrecht, I. A. Hussein and M. H. El-Naas, DOI: **10.2139/SSRN.4570278**.
137 C. A. Coutinho and V. K. Gupta, *J. Colloid Interface Sci.*, 2007, **315**, 116–122.
138 M. Todica, T. Stefan, D. Trandafir and S. Simon, *Cent. Eur. J. Phys.*, 2013, **11**, 928–935.
139 S. Temel, E. Yaman and F. O. Gökmen, *AIP Conf. Proc.*, 2018, **2042**(1), DOI: **10.1063/1.5078935/773398**.
140 Y. S. Li, Y. Han, J. T. Qin, Z. Y. Song, H. H. Cai, J. F. Du, S. F. Sun and Y. Liu, *J. Appl. Polym. Sci.*, 2016, **133**, 44150.
141 R. R. Mansurov, I. A. Pavlova and A. P. Safronov, *ChemistrySelect*, 2022, **7**(47), e202202775.
142 B. Ari, S. B. Sengel and N. Sahiner, *SPE Polym.*, 2021, **2**, 97–109.
143 J. Yun, J. S. Im, A. Oh, D. H. Jin, T. S. Bae, Y. S. Lee and H. Il Kim, *J. Mater. Sci. Eng. B*, 2011, **176**, 276–281.
144 C. Su, A. K. Berekute and K. P. Yu, *Sustainable Environ. Res.*, 2022, **32**, 1–15.
145 S. Banivaheb, S. Dan, H. Hashemipour and M. Kalantari, *J. Saudi Chem. Soc.*, 2021, **25**, 101283.
146 M. M. Eshaghi, M. Pourmadadi, A. Rahdar and A. M. Díez-Pascual, *J. Drug Delivery Sci. Technol.*, 2023, **81**, 104304.
147 S. Mallakpour and N. Mohammadi, *Carbohydr. Polym.*, 2022, **285**, 119226.
148 Y. Guo, S. Chen, Y. Yu, H. Tian, Y. Zhao, J. C. Ren, C. Huang, H. Bian, M. Huang, L. An, Y. Li and R. Zhang, *J. Am. Chem. Soc.*, 2019, **141**, 8407–8411.
149 M. Pal, J. G. Serrano, P. Santiago and U. Pal, *J. Phys. Chem. C*, 2006, **111**, 96–102.
150 Y. Ding, I. S. Yang, Z. Li, X. Xia, W. I. Lee, S. Dai, D. W. Bahnemann and J. H. Pan, *Prog. Mater. Sci.*, 2020, **109**, 100620.
151 Y. Nur, J. R. Lead and M. Baalousha, *Sci. Total Environ.*, 2015, **535**, 45–53.
152 M. Shahid, Z. H. Farooqi, R. Begum, M. Arif, A. Irfan and M. Azam, *Chem. Phys. Lett.*, 2020, **754**, 137645.
153 P. Patel, P. Gangwar and P. Thareja, *J. Vinyl Addit. Technol.*, 2023, **29**, 773–794.

154 R. Mansurov, I. Pavlova, P. Shabadrov, A. Levchenko, A. Krinochkin, D. Kopchuk, I. Nikonov, A. Prokofyeva, A. Safronov and K. Grzhegorzhevskii, *Inorganics*, 2023, **11**, 92.

155 N. Gao, W. Xie, L. Xu, Q. Xin, J. Gao, J. Shi, J. Zhong, W. Shi, H. Wang, K. Zhao and L. Lin, *Int. J. Biol. Macromol.*, 2023, **253**, 126367.

156 X. Han, J. H. Lin, X. Y. Zhang, H. K. Peng, L. Y. Liu, L. Zhang, C. W. Lou, B. C. Shiu and T. T. Li, *Composites, Part A*, 2024, **176**, 107858.